Carbon Fibres from Victorian Lignite

Final Report – Public Version

September 2020

Mamun Mollah[1], Sobhan Fakhrhoseini[2], Ramdayal Yadav[2], Alan Chaffee[1], Minoo Naebe[2]

[1] School of Chemistry, Monash University, Victoria 3800, Australia

[2]Institute for Frontier Materials, Carbon Nexus, Deakin University, Geelong 3220, Australia

Executive Summary

The ambitious aim of this project is to produce carbon fibre (CF) from Victorian lignite (VL) derived feedstock. A series of VL derivatives were prepared for evaluation as CF precursors, the details of which have been redacted from this public report.

The derivatives were characterised by ultimate analysis (CHN), Fourier transform infrared spectrometry (FTIR) and thermogravimetric and differential thermal analysis (TGA-DTA). Some samples were also analysed by ^{1}H NMR and ^{13}C NMR.

In order to understand the spinnability of developed lignite samples, two different methodologies have been employed: electro-spinning and wet-spinning. Electro-spinning of Victorian lignite derivatives-PAN blends was carried out to understand the miscibility of these two components in solvents and tendency of the polymeric dope to form fibres. The spinning of different blends and their products was investigated using the electro-spinning method during the first and second quarters of this project; following this the decision was made to fabricate continuous wet-spun fibres from selected products. Therefore, a range of derivative-PAN blends were prepared and wet-spun to obtain precursor fibres which were tested for their mechanical performance. Although the mechanical properties of the fibres obtained from the blends were generally reduced by the addition of lignite derivatives, the optimization of wet-spinning parameters gave precursor fibres with comparable mechanical properties to that of pristine PAN precursor fibre.

To develop carbon fibre, the obtained precursor fibres from wet-spinning must be stabilized under air atmosphere to form a ladder-like structure within the fibre. The stabilization process prepares the fibre for subsequent heat treatment in the high temperature environment. To obtain optimized stabilization and carbonisation conditions, the VL derivative-PAN blended fibres were first stabilized at varying temperature, under tension in air, followed by low temperature carbonisation. These factors were appropriately varied and subsequently optimized; then, the stabilized fibres were carbonised at low temperature. The mechanical properties of the carbonised fibre were evaluated by a single fibre mechanical test (Favimat). Apart from the mechanical properties of the carbonised CF, the development of crystallinity and microstructure also influences its final properties. Therefore, X-ray diffraction (XRD) and RAMAN analysis were conducted on the fibres to reveal their micro and crystallographic structure.

Due to practical limitations at lab scale, the CF developed in the current study was low temperature (LT) carbon fibre and demonstrated comparable mechanical properties to the many other reported LT carbon fibres. It is concluded that the utilization of VL in PAN as CF precursor has a huge potential for alternative low-cost CF precursor material.

Table of Contents

Introduction

Carbon fibre (CF) is a strong and lightweight material with excellent thermal and chemical resistivity. Mechanical properties and surface functionalities of carbon fibres can be tailored to produce fibres with a broad range of tensile strength and modulus compatible with either thermoset or thermoplastic matrices. It also can be designed into unidirectional fibre tapes or fabrics, woven fabrics, non-woven mats, chopped or even milled fibres for different applications. Popularity of carbon fibre reinforced polymers (CFRPs) against traditional materials such as steel and aluminium in aerospace, civil engineering, the military, automotive and sports equipment industries is increasing because of its high rigidity, tensile strength and chemical resistance combined with low weight (Alcañiz-Monge et al., 1997; Frank, Steudle, Ingildeev, Spoerl, & Buchmeiser, 2014). However, its application is limited to niche products due to its high cost. More than 90% of commercial carbon fibre in the market are made from PAN precursor and it is well known that cost of precursor material is the major contributing element in carbon fibre cost (Khayyam et al., 2020). Figure 1 shows the cost breakdown chart for PAN-based carbon fibres. This figure might slightly change on account of varying oil price and the production capacity of individual companies.

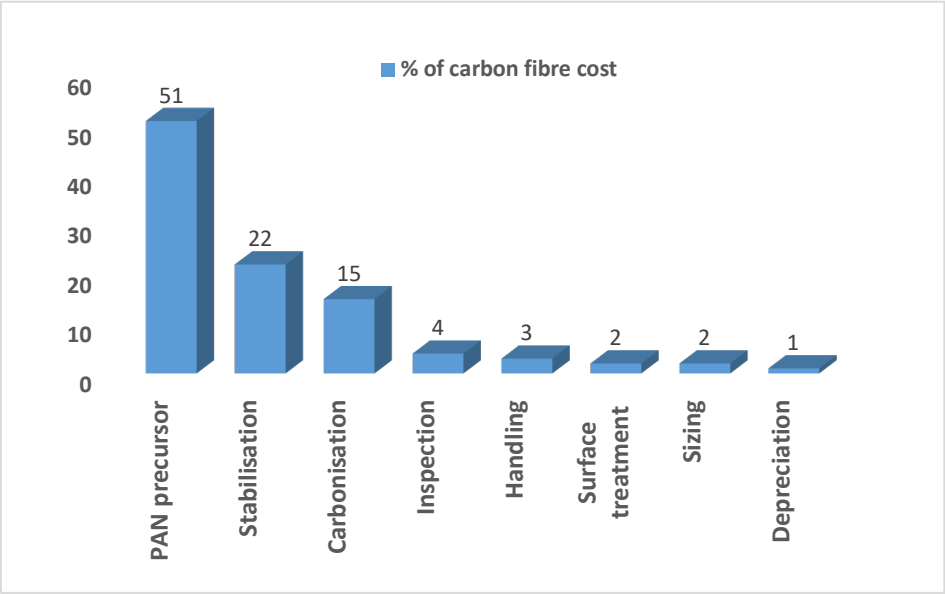

Figure 1 Cost break-down chart for processing PAN precursor to carbon fibre(Nunna, Blanchard, Buckmaster, Davis, & Naebe, 2019)

To reduce the price of carbon fibre, alternative precursor materials such as cellulose coal tar and petroleum pitch and lignin have been investigated (Jiang et al., 2019; Oroumei, Fox, & Naebe, 2015; Zabihi et al., 2019). Victorian lignite (VL) is particularly attractive, because of its low level of inherent inorganic impurities as well as its low price.

1. Derivatives from Lignite

The methods used to prepare derivatives from VL are not disclosed in this public report, but are described in the confidential report provided to ACI. The various VL derivative samples described in this report are given the following code names, which refer to the original sample and the treatment method:

Sample 1

Sample 1_1

Sample 1_2

Sample 1_3

Sample 1_4

Sample 2

Sample 3

Sample 4

Sample 5

Sample 6

2. Spinning methods to prepare precursor fibre

Converting Victorian lignite derivatives into nano- or micro-sized fibres is possible by using any of the conventional methods: (i) melt-spinning, (ii) electro-spinning and (iii) wet-spinning. Each method has its own advantages and disadvantages, as are discussed in following sections.

2.1 Melt-spinning process

Melt-spinning process is applicable for the precursor materials that can be melted below their degradation temperature. In this method the precursor material is melted and extruded through the holes of spinneret, solidified by passing a free length in air and finally, melt-spun fibres are collected on a collector.

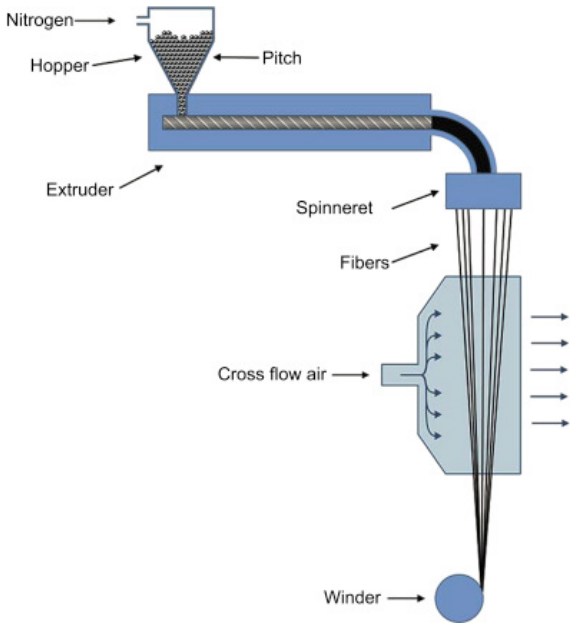

Figure 2 Schematic of melt-spinning process and different parts of the process

High production rates and solvent-free spinning are two main advantages of this process that reduce the cost of precursor manufacturing. However, extra purification and thermal processing steps are required to prepare tar-based materials for melt-spinning. The main aim of further thermal processing is to convert isotropic pitch into mesophase pitch with high liquid crystallinity that form fibres with high domain size and alignment at melt-spinning. In other words, as-received tar pitch with smaller crystallite domains will produce low-grade precursor fibres that are able to make general purpose carbon fibres, not even suitable for automotive grade applications. Increasing mesophase content of tar pitch requires capital investments and it may not be feasible for making automotive grade carbon fibres.

2.2 Electro-spinning process

The electro-spinning method has the ability to process different polymers, polymer blends or filler loaded polymers to fabricate fibres with desired sizes and tailored morphology and pore structure. The team at Deakin University has been conducting several research projects on fabrication of nanofibres from polyacrylonitrile (PAN), PAN/lignin, poly caprolactone (PCL), poly vinylidene fluoride (PVDF) and PAN/bituminous coal derivatives nano-fibre mats using electro-spinning technique. The principle of electro-spinning fabrication method is to apply an electric force between polymer dope at the tip of a nozzle and the collector. Figure 3 demonstrates a schematic of the lab-scale electro-spinning set up that is used in this project.

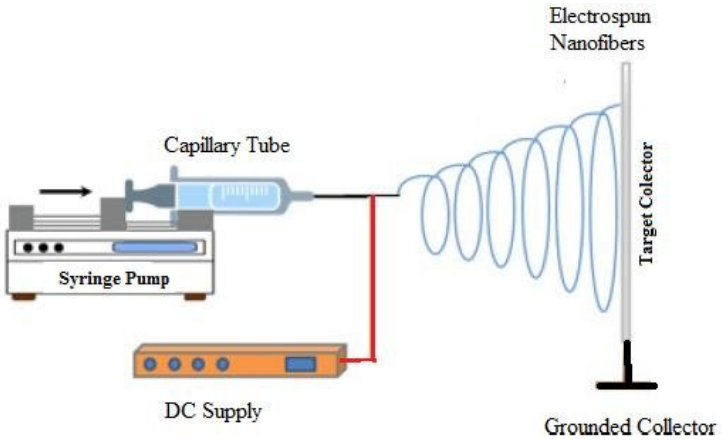

Figure 3 Schematic of a lab-scale electro-spinning set-up

Electro-spinning is a quick method to understand mixing behaviour of two polymers and stability of polymeric mixture in fibre formation process. This method is suitable for preparing nano-fibre mats for non-structural applications.

2.3 Wet-spinning process

In this method, a highly viscous solution is extruded through a multi-hole spinneret that is placed in a liquid bath containing non-solvent liquid. The polymer is coagulated due to diffusion of solvent from the polymeric dope into the bath and a fibre structure is formed in the coagulation bath. The main cause of fibre formation is a counter-current mass transfer of solvent from the polymeric dope to the bath and non-solvent liquid from the coagulation bath into the fibre. Figure 4 shows a schematic of how a polymeric dope solidifies into a nascent fibre in a coagulation process.

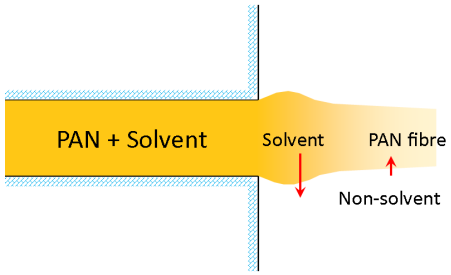

Figure 4 schematic of polymer solidification into the fibre in the coagulation bath

Further washing and hot water drawing steps remove excess solvent from the fibre and draw it multiple times to align PAN crystallites and remove voids in the fibres. Drawn fibres will dry in a hot air column, in some cases pass through an extra steam draw chamber, dry and collect in the end of process. Figure 5 shows schematic of a typical wet-spinning process for PAN-based precursor.

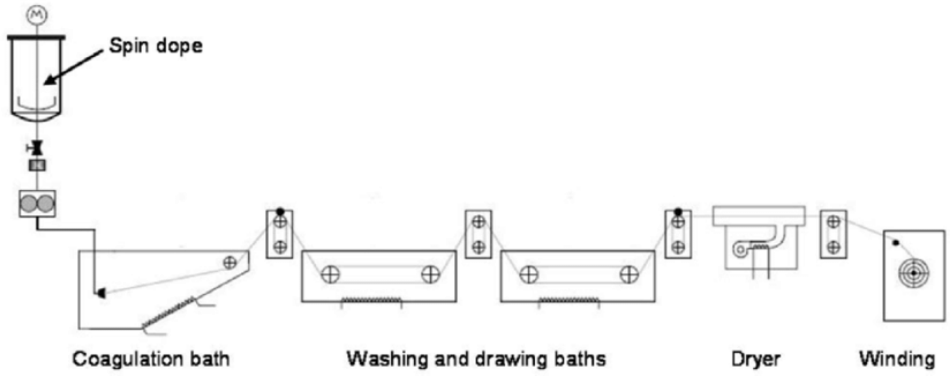

Figure 5 schematic of wet-spinning process

Wet-spinning method is a very well-established method and is used widely by manufacturers of PAN based carbon fibre precursors.

2.4 Selection of suitable spinning method

As discussed above, all methods are potentially suitable for converting lignite extract into precursor fibres. To develop a clear idea on selecting the more feasible spinning method, we listed pros and cons of each method and compared them in below:

- Electro-spinning of lignite derivatives will result in nano-fibre mats, which can be used for energy related applications; for example, in batteries and supercapacitors, but are not suitable for structural applications. This can be a preliminary approach to rapidly investigate miscibility and spinnability of lignite derivatives with and without PAN.
- Melt-spinning could be a suitable candidate to convert lignite derivatives into precursor fibre. It is a solvent free process with high production rate and suitable for thermoplastic materials. However, melt spinning high quality precursor fibres with uniform mechanical properties is not achievable without preliminary thermal processes. Combination of low molecular weight aromatics with random chemical structures in unprocessed lignite derivatives causes instability of melt viscosity at spinning temperature. This can result in axial heterogeneity of diameter and mechanical properties in precursor fibre and may disrupt the spinning process. Furthermore, melt-spun fibres can be very brittle and hard to handle. In addition, thermal stabilisation of some lignite derivative fibres is expected to be very slow due to thermoplastic behaviour. This is similar to thermoplastic fibres such as cellulose, lignin and pitch-based fibres that need to be thermoset before processing at higher temperature. All preliminary thermal treatment of lignite material and thermal stabilisation of melt-spun fibres require a significant capital investment.
- Wet-spinning is a solvent-based spinning process and requires a polymeric matrix with high molecular weight to increase viscosity and subsequently spinnability of solution. Low viscosity

of lignite derivatives might limit the amount of filler in the spinning dope and reduce the cost-saving potential of the new product. However, the wet-spinning method is the most globally accepted process for manufacturing carbon fibre precursor. Therefore, the required infrastructure and knowledge are available in a majority of fibre production companies. Moreover, adding lignite derivatives or any other lignite product into a polymeric matrix is does not require any additional capital investment and should be economically feasible.

As such, in this research project, at the beginning we selected electro-spinning method as a preliminary technique to investigate miscibility and spinnability of lignite derivative-/PAN mixture with different lignite derivatives and compositions. Then, based on our observations of electro-spinning behaviour and performance, several lignite derivatives were selected for wet-spinning.

3. Experimental procedure to develop precursor fibre for final CF

Electro-spinning method was first selected as a screening method to investigate spinnability of 100% lignite derivatives or its blends with PAN polymer. Then, a number of spinnable lignite derivative samples were selected for further investigation by the wet-spinning method. Finally, wet-spun precursor fibres were converted into carbon fibres through thermal stabilisation and carbonisation steps. To produce nano- and micro-fibres, VL samples were tested and screened to identify the VL product with highest potential to form CF-grade precursor fibres. Details of sample preparation and experimental condition of each step is described in next sections.

3.1 Electro-spinning experiments

To obtain the suitable electrospinning parameters for spinning of VL derivatives-PAN, a range of experimental parameters including applied voltage, dope concentration, spinning distance were tested. **Error! Reference source not found.**All the electrospun samples were collected and dried on aluminium foil in air at room temperature.

3.2 Wet-spinning experiments

In order to explore the potential of lignite-based fibres in structural applications, wet-spinning method was used to produce continuous precursor fibres. Figure 6 shows the wet-spinning equipment at Deakin University, which was used for this project.

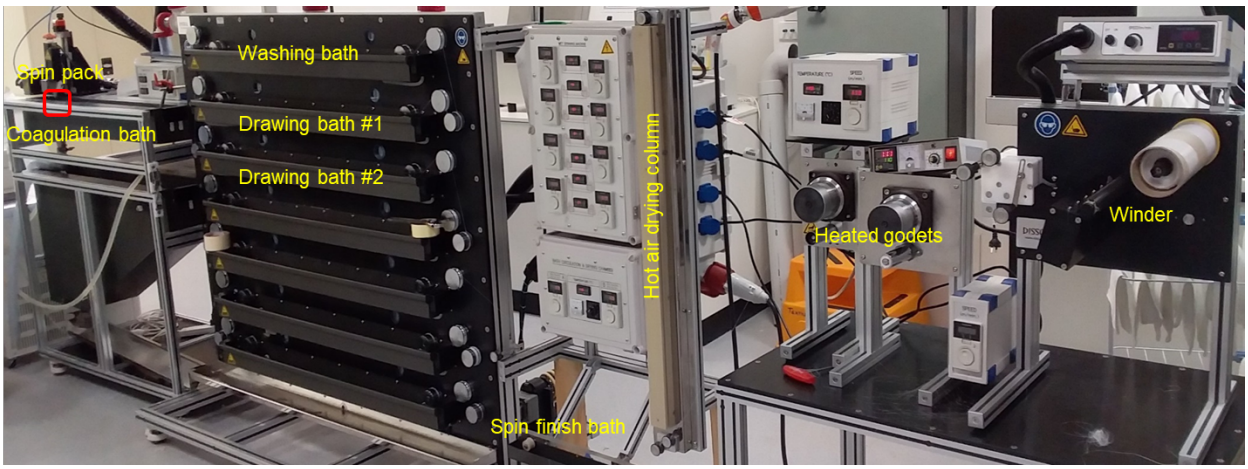

Figure 6 Image of wet-spinning set-up at Deakin University

As shown in Figure 6, the wet-spinning equipment contains multiple sections. To produce a quality precursor fibre with reliable physical and mechanical properties a detailed optimisation of processing parameters is required. The various sections of the wet-spinning unit are briefly explained below:

1- **Temperature controlled spin pack**: It is important to maintain temperature of the spinning dope within a certain range to prevent phase separation and also to reduce dope viscosity. Based on our previous experiences on wet-spinning, the temperature of spinning dope is an important parameter as it influences the flow behaviour of dope.

2- **Extrusion rate at the spin pack**: Wet-spinning at very low shear rate damages the alignment of polymeric chains in the fibre. Extrusion at very high shear rate also increases the risk of phase separation as the two materials (for example PAN and Sample 1) have different responses to a high shear flow. Therefore, to spin fibres with desired mechanical properties and without inter-filament fusion, an optimum range of extrusion rates needs to be considered.

3- **Spinneret**: It is very important to select a multi-filament spinneret to investigate the uniformity of extruded filaments across a tow. We used a 100 filaments spinneret for this set of experiments.

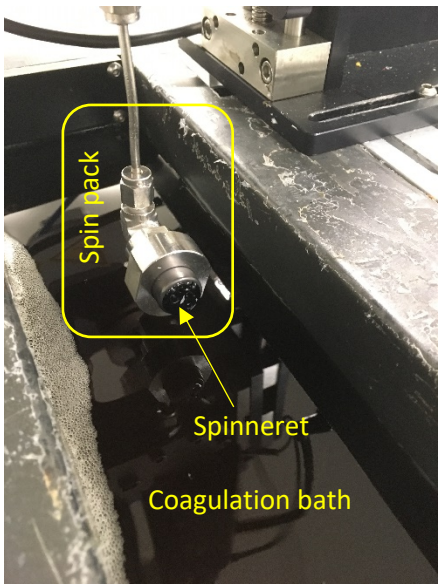

Figure 7 A close-up shot of spin pack and coagulation bath

4- **Coagulation bath**: Extruding spinning dope into a 100% non-solvent coagulation bath make fibres brittle and leaves many voids in fibre. The reason is a high counter-current mass transfer between spinning dope and non-solvent part in the coagulation bath. To control mass transfer rate and minimise void formation, spinning dope is extruded into a solution of solvent and non-solvent in the coagulation bath. Moreover, a high coagulation rate results in a bean (or known as kidney) cross-sectional shape, which might not be desirable for some applications. Therefore, by adjusting solvent/non-solvent ratio in the coagulation bath and controlling coagulation rate, fibres with desired cross-sectional shape and with less void will be produced. Below schematic shows the coagulation mechanism in the coagulation bath.

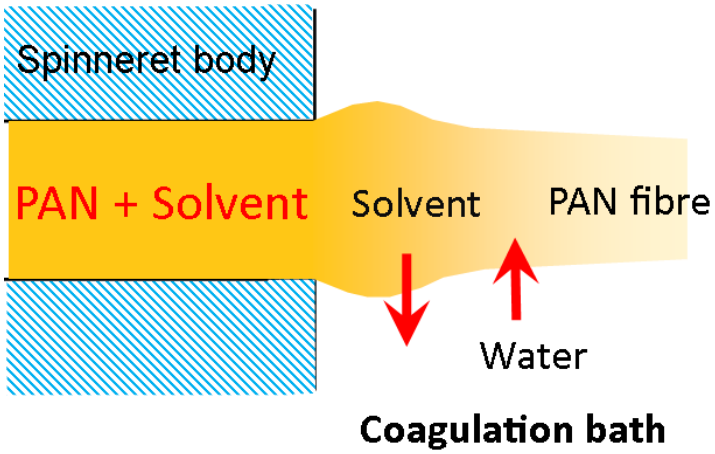

Figure 8 Schematic of fibre formation mechanism after extrusion of the spinning dope into coagulation bath

5- Washing of pristine fibre in washing bath is a compulsory step to remove extra solvent form the surface of fibres. This process usually takes place in a 100% non-solvent bath without applying any tension on fibres.

6- **Hot water drawing bath**: After washing wet-spun fibres, the nascent tow passes through a number of hot water baths and tension is applies onto the fibres. This is to align the polymer chains along the fibres' axis so as to improve their mechanical properties.

7- **Spin-finishing bath**: The spin-finish is an amino-silicon water soluble chemical that covers surface of fibre to reduce the electro-static entanglement between filaments, protect fibres at higher temperatures, and prevent fusion of filaments into each other at the drying stage.

8- **Hot airdrying column**: This is used to evaporate surface water that is carried out by tows at different stages.

9- **Heated godet rollers**: These dry the fibres and make them ready for winding.

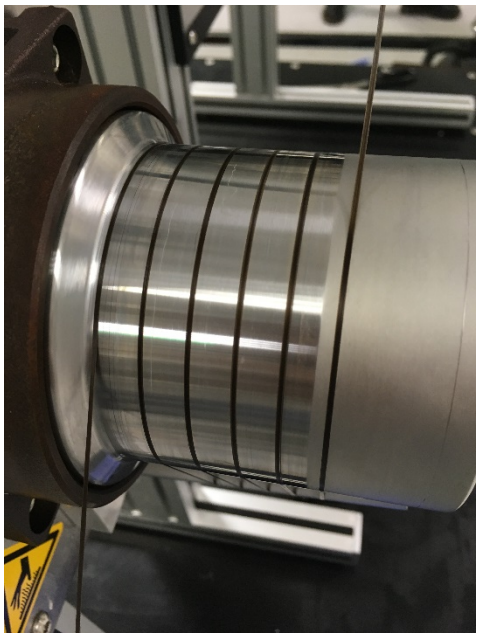

Figure 9 A close-up shot of heated godet with 20wt% Sample 1_1/PAN fibres

10- **Winder**: Winding is the last stage of precursor fibre production and at this stage dried wet-spun tow is collected under a certain tension.

As stated earlier, in order to spin fibres with acceptable mechanical properties, the wet-spinning processing parameters associated with all the above components were optimized and kept constant for throughout the wet spinning process.

3.3 Thermal conversion of wet-spun fibres

Stabilization of 100 filaments precursor tows proceeded in a fan forced oven by hanging a weight on one end to keep fibres under tension, as shown in Figure *10*. Three different sets of stabilized fibres were prepared in the temperature range of 180℃-300℃. The effect of processing temperature on the extent of stabilization reaction (EOR) value was investigated, making use of the following equation:

$$EOR = \frac{0.29 \times Abs_{1595}}{Abs_{2243} + 0.29 \times Abs_{1595}}$$

Where:

Abs_{1595} is intensity of FTIR peak at 1595 cm^{-1}, which belongs to –C=N- and identifies progress in cyclisation reaction

Abs_{2243} is intensity of FTIR peak at 2243 cm^{-1}, which belongs to -C≡N and identifies amount of unreacted nitrile groups in PAN polymer chain

Figure 10 Isothermal stabilization of precursor fibres for EOR investigation

EOR values provide an indication of how stabilised fibres react at higher temperature and during carbonisation step. The preferred EOR value for a properly stabilised fibre is between 65 and 70%. Fibres with low EOR (<60%) burn or degrade in carbonisation furnace and over-stabilised fibres (EOR>70%) will not result in carbon fibres with high mechanical performance. In the given conditions, the wetspun fibers were stabilized and then transferred to a tube furnace for low temperature carbonisation. Carbonisation of 1000 filaments of stabilised fibres was completed in a tube furnace.

As for the stabilisation step, a range of weights were suspended from one end of tow to keep fibres under tension during carbonisation. Figure 11 shows pictures of the large fan forced oven and tube furnace that were used for stabilisation and carbonisation of 1000 filament tows.

Figure 11 Picture of fan-forced oven and tube furnace

After low temperature carbonisation, fibres were collected to investigate the effect of stabilisation and carbonisation tensions on their mechanical properties. Then, the optimum condition was used to carbonise fibres at higher temperature and make HT carbon fibres.

4. Characterization

4.1 Characterization of VL derivatives

For solubility observation, small amounts (e.g. 5g) of VL derivative was mixed with about 3 mL of solvent and ultrasonicated. The extent of solubility was estimated by examination of the visual appearance of the mixture. The elemental analyses were carried out using a PerkinElmer CHN2400 CHNS analyser. ATR-FTIR was carried out using an Agilent Cary 630 FTIR spectrometer on ground sample.

Helium density: The helium densities of the samples were determined on dried samples by helium pycnometry using an AccuPyc 1330 model pycnometer (Micromeritics, Norcross, GA, USA). The unit was calibrated on a daily basis.

Surface area: Surface area was measured by CO_2 adsorption using a Micromeritics TriStar II 3020 analyzer at 0 °C. CO_2 surface areas and micropore volumes (pores <2 nm diameter) were calculated using the Dubinin–Radushkevitch (DR) equation.

NMR: For ^{1}H NMR, spectra were obtained at room temperature using a Bruker Ultrashield 400 MHz instrument with a 90 ° pulse flip angle (9.5 µs). Solid state ^{13}C NMR spectra were recorded at room temperature using a Bruker Avance 400 spectrometer.

To aid interpretation, ^{1}H NMR spectra were divided into four regions (Charlesworth, 1980; Peter. J. Redlich, 1987): protons attached to aromatic rings (H_{ar}, 6−9 ppm); protons attached to aliphatic carbon adjacent to aromatic rings (H_{α}, 4.5−1.96 ppm); protons attached to carbons further away from aromatic rings (methylene protons) and protons of paraffin groups (H_{β}, 1.95−1 ppm); and protons in CH_3 groups (H_{γ}, 1−0.5 ppm). In an analogous manner, the ^{13}C NMR spectra were divided into multiple regions, as suggested by Kelemen et al (Kelemen et al., 2007). The proportions of the four hydrogen types and the different carbon types were determined using Bruker's Topspin 3.1 software. The fraction of aromatic carbon in the asphaltenes, tar and pitch was calculated using the Brown-Ladner equation (Brown & Ladner, 1960; Wilson, 1981) from the elemental analysis (Table 1) and the ^{1}H NMR (not shown). The fraction of aromatic carbon in the VL was calculated from the solid state ^{13}C NMR (Wilson, 1981) spectrum.

TGA: Samples were analysed in a thermogravimetric balance for weight loss (TG), derivative of weight loss with respect to temperature (DTG) and heatflow (DTA) using a Setaram TAG24 symmetrical thermoanalyser. Three reaction conditions were used, N_2 to 800 C, air/N_2 (50:50, v/v) to 800 °C and air/N_2 (50:50, v/v) to 300 °C. The gas was dosed into the thermoanalyser using Bronkhorst programmable mass flow controllers.

The mass loss calculated using the equation below:

$$\text{Mass loss} = [(M1 - M2) / m1] \times 100$$

Where, M1 was the original test sample weight before experiment and M2 was sample weight after experiment.

The ash yield was calculated from the air/N_2 experiment to 800 °C by the equation below:

$$\text{Ash yield} = M2/M1 \times 100.$$

The uncertainty based on duplicate determinations was about +/-2% for mass loss and ash yield.

4.2 Analysis of fibres

Scanning electron microscopy (SEM) imaging was carried out to observe surface morphology of electro-spun fibres. Physical and mechanical properties of wet-spun fibres were measured with a Favimat Air-Robot single fibre tester. Differential scanning calorimetry (DSC) and thermogravimetric analysis (TGA) methods were applied for thermochemical analysis of fibres, including the investigating of any possible interaction between PAN and filler material at higher temperatures. Extent of reaction (EOR) values for the stabilised fibres were calculate based on ATR-FTIR measurement. The developed CF has been studied with X-ray diffraction and Raman spectroscopy to obtain the crystallographic and structural details.

5. Results and discussion

5.1 VL derivatives

Solubility test: Solubility tests were conducted for mixing the precursor material with PAN was determined qualitatively, by visual observation.

Proximate and ultimate analyses: Table 1 gives proximate and ultimate analyses of the coking coal tar pitch and VL tar as examples of the analyses that were carried out. Conclusions were drawn about the nature of the materials. Further details are redacted from this public report.

Table 1: Proximate and ultimate analyses.

Sample						Moisture	Ash Yield	Oxygen
	C	H	N	S	H/C	(wt%)	(Wt%db)	(Wt%db, by diff)
Pitch (Coking coal)	93.02	4.36	1.36	0.40	0.56	-	0.4	0.47
VL tar	74.01	9.36	0.62	0.40	1.51	-	0.3	15.32

Helium density: Details are redacted from this public report.

Surface area: Details are redacted from this public report.

NMR: Table 2 shows structural parameters determined by solid state ^{13}C NMR from the spectra. Details are redacted from this public report.

Table 2: Structural parameters determined by solid state ^{13}C NMR.

[a] number of carbons in average aliphatic chain.
[b] number of carbons in average aromatic cluster.
[c] atomic percent.

Description	Symbol	chemical shift range or definition
Aromatic/carboxyl/carbonyl/amide	fa	90-240
Aromatic	fa'	90-165
Carboxyl/carbonyl/amide	fa^{C}	165-240
Protonated aromatic	fa^{H}	110-128
non-protonated aromatic	fa^{N}	$fa'-(fa^{H}+fa^{P}+fa^{S})$
Phenoxy/phenolic	fa^{P}	150-165
AlkyL-substituted aromatic; biaryl	fa^{S}	135-150
bridgehead aromatoc	fa^{B}	128-135
aliphatics	fal	0-90
methylene/methine	fal^{H}	(22-90)-(50-60)
methyl/methoxy	fal'	(0-22)+(50-60)
alcohol/ether	fa^{O}	50-90
fraction of aromatic carbons with attachments*	FAA	$(fa^{P}+fa^{S})/fa'$
average aliphatic carbon chain length*	Cn'^{a}	fal/fa^{S}
fraction of methyl in aliphatic*	FMA	fal'/fal
average carbon per aromatic cluster*	C^{b}	x axis value against kai b value in Fig 6
lower limit estimate for organic oxygen*	$LLEOO^{c}$	$fa^{C}+0.5(fa^{P}+fa^{O})*100$

FTIR spectra were obtained but are redacted from the public report.

TGA experiments under N_2 at 800 °C: Figure 12 and Figure 13 show TGA and DTG curves respectively of the different materials. As expected, pre-treatment at higher temperature tended to reduce the volatility of the materials but it did not change the temperature range where the main mass loss occurred (see Figure 12). When the materials were subjected to treatment 1 rather than treatment 2, the main weight loss step in the TGA was shifted to higher temperatures. This suggests that treatment 1 changed some of the components of the Sample 1 variants to make them more thermally stable. Sample 2 and 3 showed similar weight loss curves. Sample 6 was less volatile than Sample 1 variants and the mass loss occurred over a much smaller temperature range, suggesting the range of components was smaller than for the Sample 1 variants. This higher carbonization yield of Sample 6 would be expected from its distinct chemical structure other factors such as average molecular weight being constant (Ko, Choi, Lee, & Jeon, 2017). However, chemical structure is not always correlated with low volatility; the Sample 1 variants had higher aromaticity than Samples 2 and 3 but also higher volatility, so that other factors must also be important. The Sample 1 variants and Sample 2 showed much less symmetrical DTG peaks than Sample 6 with the low temperature side extending over a much wider range of temperature than the high temperature side (Figure 13). Thus, each kind of material showed a distinct shape for the main DTG peak.

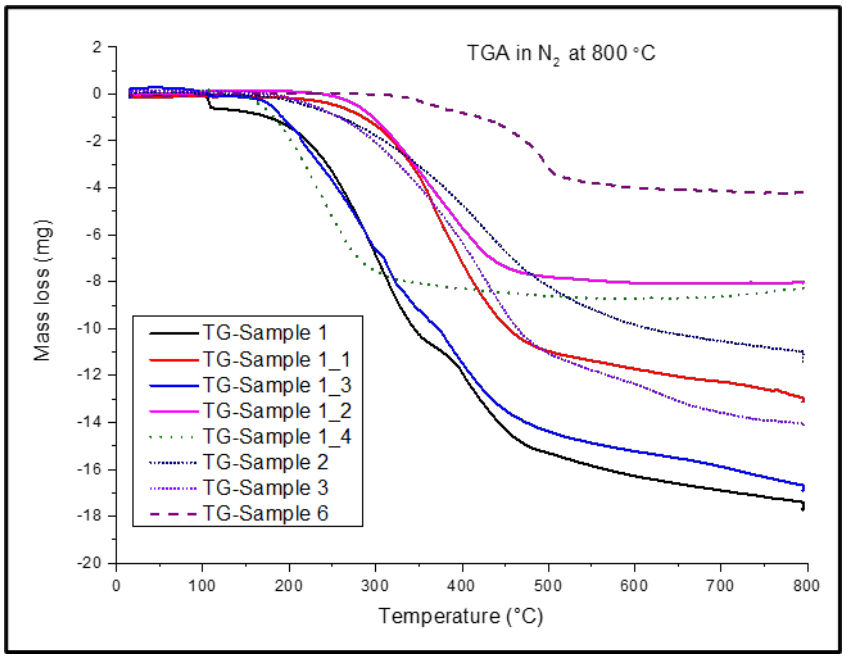

Figure 12: TGA curves under N_2 up to 800 °C.

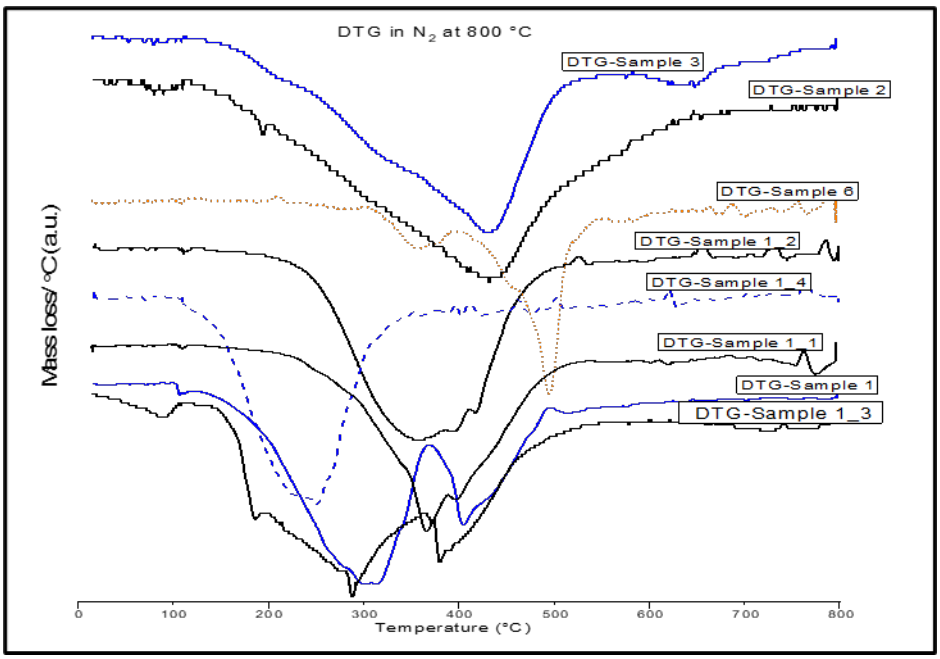

Figure 13: DTG curves under N_2 up to 800 °C.

For the Sample 1 variants the DTA (Figure 14) indicated clear distinction between different treatments. For the original Sample 1 and some of its variants subjected to treatment 1 occurred below the temperature range of volatilization. Treatment 2 led to a large decrease in the heat of reactions below the temperature range where volatilization occurred. Treatment 1 at a higher temperature also, not surprisingly, reduced the heat of low temperature reactions (since they presumably had already occurred). For treatment 2 at high temperature, reactions below the volatilization temperature range again involved more heat than those associated with volatilization. These results emphasize the complexity of the pyrolysis reactions and the important effects of drying atmosphere and temperature. The Sample 6 reactions started releasing heat at a higher temperature than the Sample 1 variants but again most of the heat observed by DTA was for reactions before volatilization occurred, emphasizing the importance of the pre-volatilization reactions. For Sample 2 and 3 most of the heat of reaction was associated with reactions occurring below the temperatures where most of the volatilization occurred.

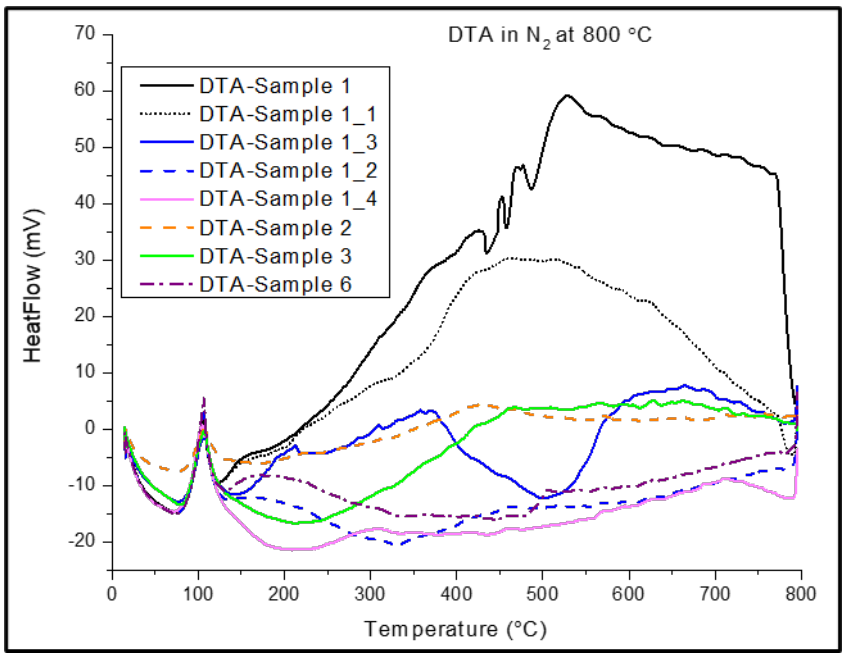

Figure 14: DTA curves under N_2 up to 800 °C.

TGA experiments under air/N_2 (1:1 v/v) at 800 °C: Figure 15 and Figure 16 show the TGA and DTG curves respectively. Overall Samples 2 and 3 lost mass more slowly than the Sample 1 variants but Sample 6 lost very little mass at low temperatures compared to the other materials. Treatment 2 tended to reduce the mass loss. Conversely to what was observed for TGA under N_2 (Figure 12) treatment 1 gave products which were more resistant to pyrolysis but combusted more easily. This may provide insight into what compound were formed during treatment 1 this method drying (low or high temperature). Compared to pyrolysis under N_2, pyrolysis under air gave much narrower DTG peaks for the Sample 1 variants (Figure 16). Treatment 2 rather than treatment 1, shifted the sharp DTG peak to lower temperatures and divided them into three distinct regions. The broad high temperature volatilization peak in 350-450 °C remained unchanged. The shape of the DTG peaks was similar for the other products tested, but treatment 1 shifted the peaks to slightly lower temperatures. The shape of the DTG peaks below 450 °C was different from that for pyrolysis under N_2 even though combustion probably did not occur at these temperatures. Preliminary reactions in air must have occurred to change the chemical structure of the materials compared to what occurred under N_2. The DTG for Sample 2 is also different to that under N_2 and there was a clear distinction between Sample 2 and 3. Sample 2 showed a single broad peak near 400 °C which was split into several components for Sample 3, more distinctive division of the components into several classes. These differences can be explained with the assistance of the DTA data.

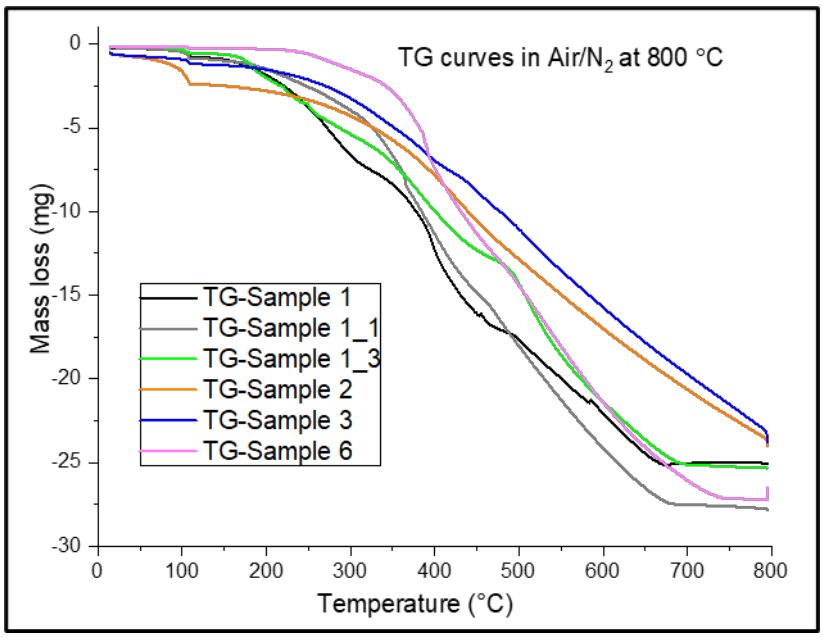

Figure 15: TGA curves under air/N_2 (1:1 v/v) up to 800 °C.

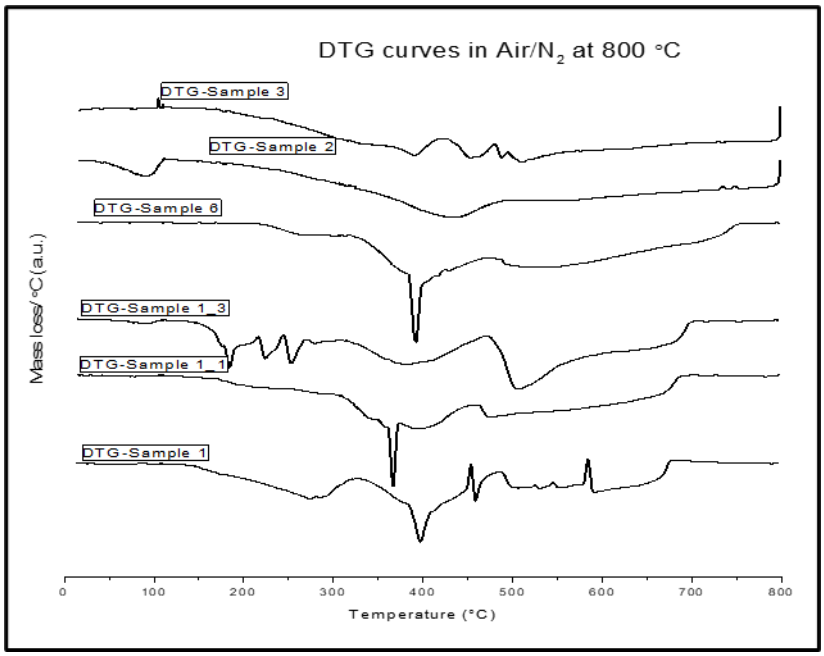

Figure 16: DTG curves under air/N_2 (1:1 v/v) up to 800 °C.

Sample 2 began to combust at 250 °C rather than above 450 °C as was the case for the other materials tested (DTA, Figure 17). This could explain the difference between Samples 2 and 3 with respect to the DTG. Treatment 1 or treatment 2 of Sample 1, reduced the temperature at which combustion began. The combustion characteristics of tar and Sample 6 were similar but the combustion of Sample 6 extended over a longer temperature range. For Sample 3 and tar and Sample 6 endothermic peaks associated with the DTG peaks below combustion temperatures were clearly distinguished.

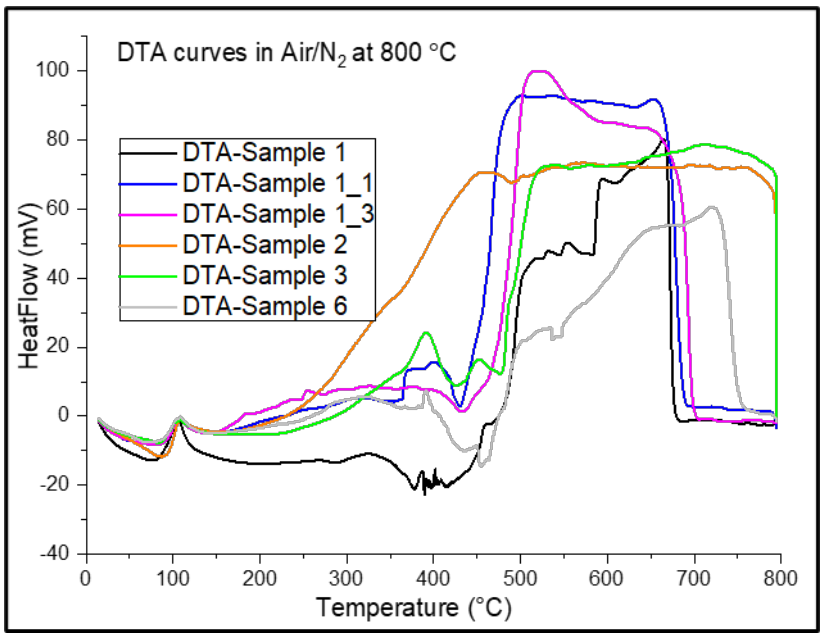

Figure 17: DTA curves under air/N_2 (1:1 v/v) up to 800 °C.

TGA experiments under air/N_2 (1:1 v/v) at 300 °C: Treatment 2 reduced the mass loss in subsequent heating in the TGA experiment and increasing the treatment temperature further reduced the mass loss heating in the TGA experiment (Figure 18). The Sample 6 and Sample 1_4 were changed to a small extent at low temperatures and subsequently were stable to 300 °C. Sample 2 lost more mass than Sample 3 and for both the mass loss proceeded over a much longer time than for the Sample 1 variants. The DTG peak structure was simple and showed the same effects as the TGA curves themselves (Figure 19).

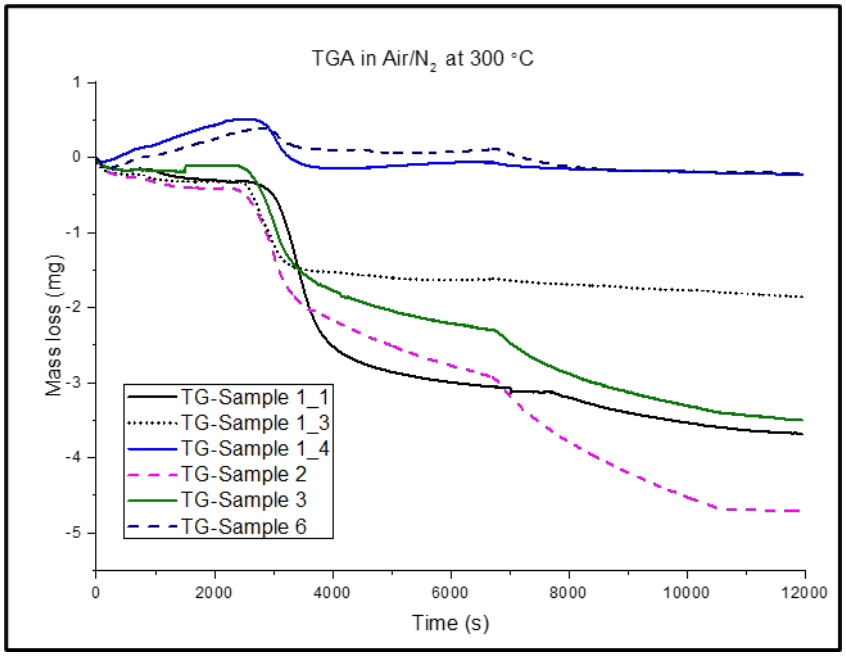

*Figure 18: TGA curves of materials in air/N_2 **(1:1 v/v)** up to 300 °C.*

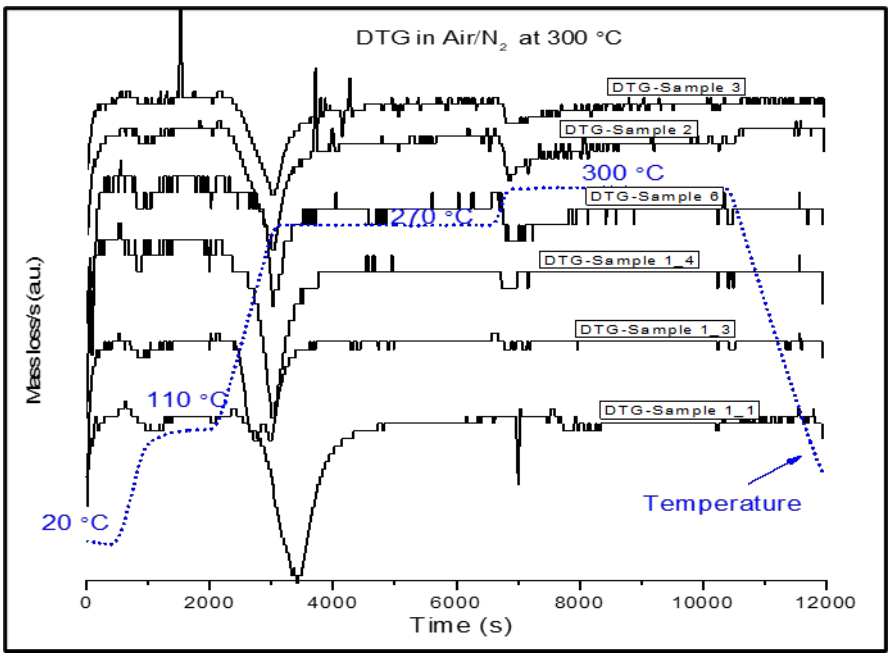

Figure 19: DTG curves under air/N_2 (1:1 v/v) up to 300 °C.

All the materials showed an endothermic peak in 150-200 °C, at too high a temperature to be associated with treatments (Figure 20). Above this the Sample 1 variants showed an exothermic peak associated with the main region of mass loss which was relatively rapid for these materials. Another exothermic peak was observed when the temperature was raised from 270 to 300 °C for all the Sample 1 variants, corresponding to reactions which only occurred at a significant rate at the higher temperature and were associated with only a small change in mass or, in the case of Sample 6, no change in mass. For Sample 2 the main mass loss reactions were significantly endothermic and extended aver a larger temperature range than the exothermic reactions responsible for the mass loss from the Sample 1 variants. The mass loss reactions for Sample 3 involved less heat flow than those for Sample 2. Again, in both cases an exothermic reaction was promoted by raising the temperature from 270 to 300 °C.

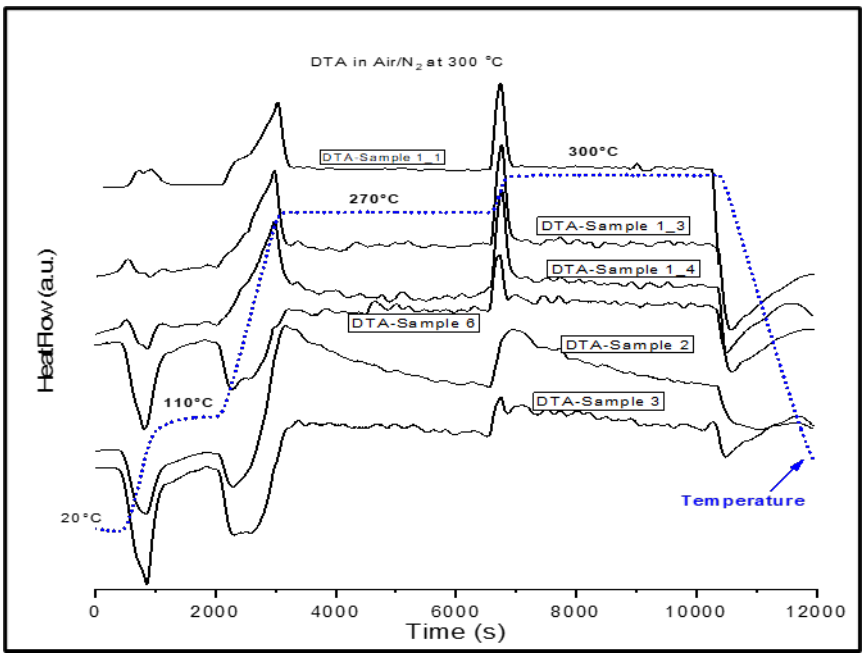

Figure 20: DTA curves under air/N_2 (1:1 v/v) up to 300 °C.

Even in the temperature range below 300 °C, a number of complex reactions varying in importance and nature with the starting material occurred. Such reactions may have important effects on the interactions between PAN and the material when they are mixed and treated.

5.2 Electro-spinning of lignite derivatives:

Figure 21 shows optical images of electro-spun mats with different Sample 1_1/PAN ratio. Nothing is visible at optical microscopy level and only visible change is change in darkness of samples with increasing lignite derivatives content.

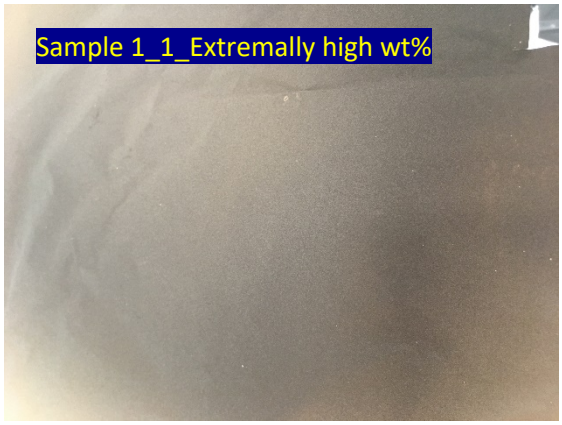

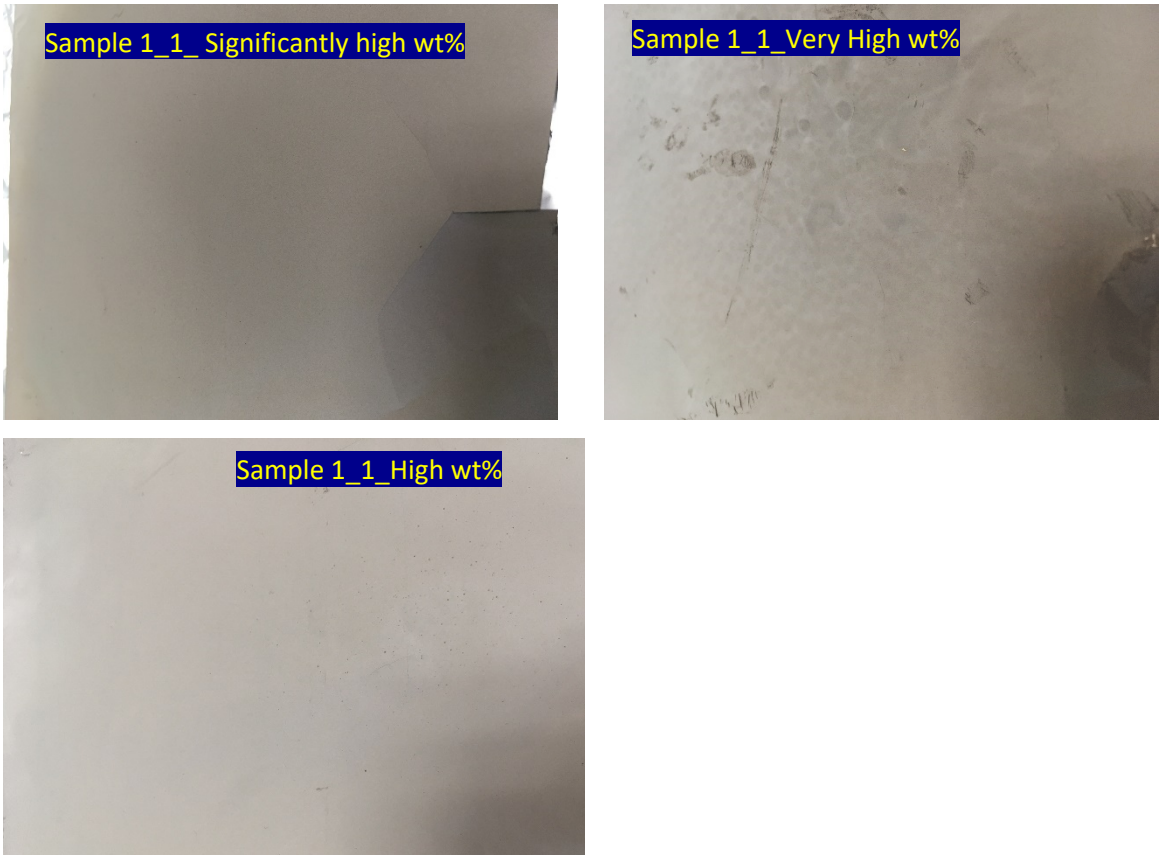

Figure 21 Optical images of different electro-spun mat containing different Sample 1_1 sample

Figure 22 provides SEM images of four different Victorian lignite derivatives samples; Sample 1, Sample 1_1, Sample 1_3 and Sample 2 without adding PAN into the dope. As shown in the images, because of very low viscosity of the dope, electro-sprayed particles appeared as a thin film rather than a nano-fibre mat.

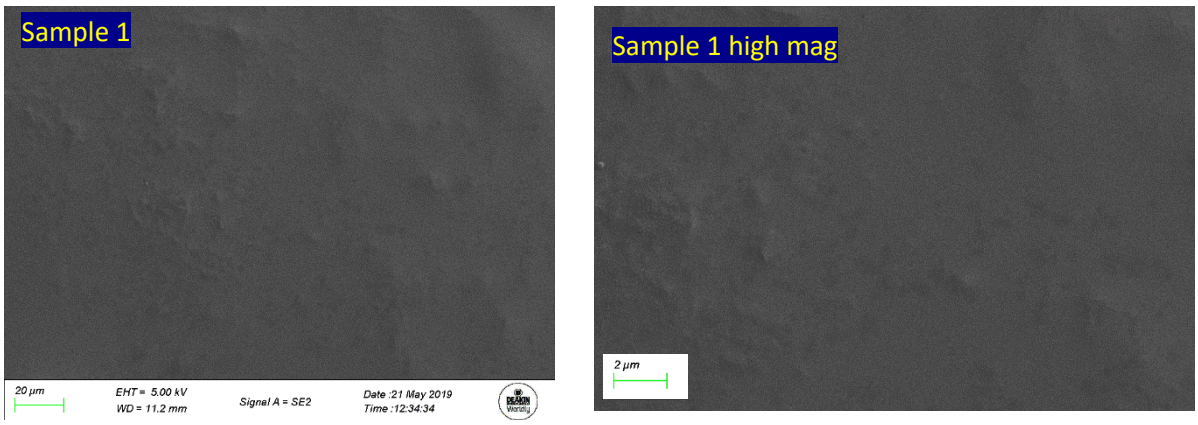

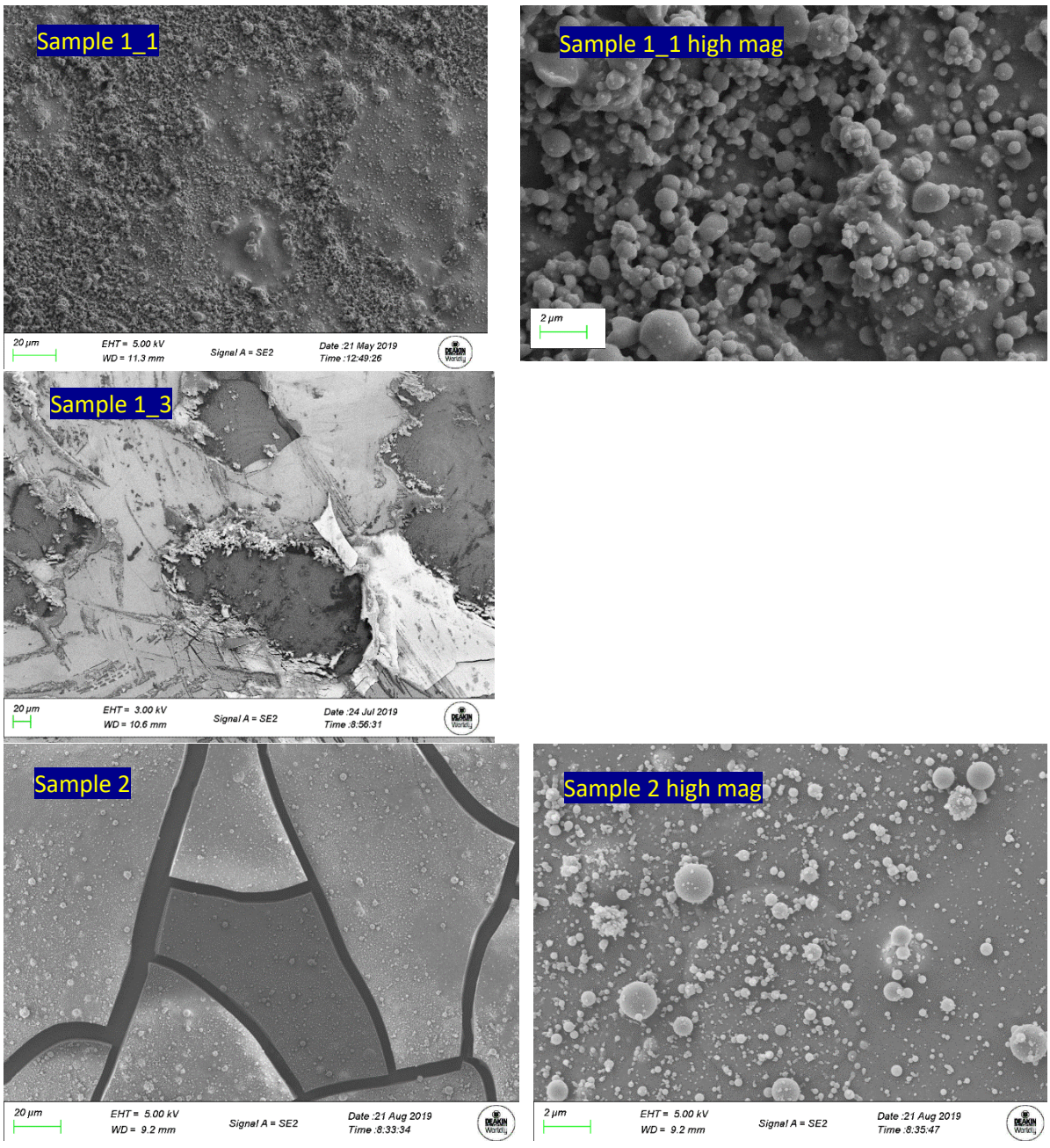

Figure 22 SEM images of electro-sprayed lignite derivatives samples

Blending PAN with Sample 1 was considered as a solution to resolve the electro-spraying issue by increasing dope viscosity. SEM images of electro-spun Sample 1/PAN nano-fibres are shown in Figure 23. Upon addition of PAN into Sample 1, a very unstable formation of fibre was observed. By adding more PAN into the dope, the fibre formation become more stable and at sufficiently high PAN proportion Sample 1/PAN blend, a stable electro-spinning process was observed, and nano-fibres were spun with uniform shape and consistent diameter across their length. However, prepared fibre mats were never dried due to liquid nature of the starting Sample 1 material. Collecting wet samples will cause major issues in wet-spinning experiment and make the unwinding process impossible.

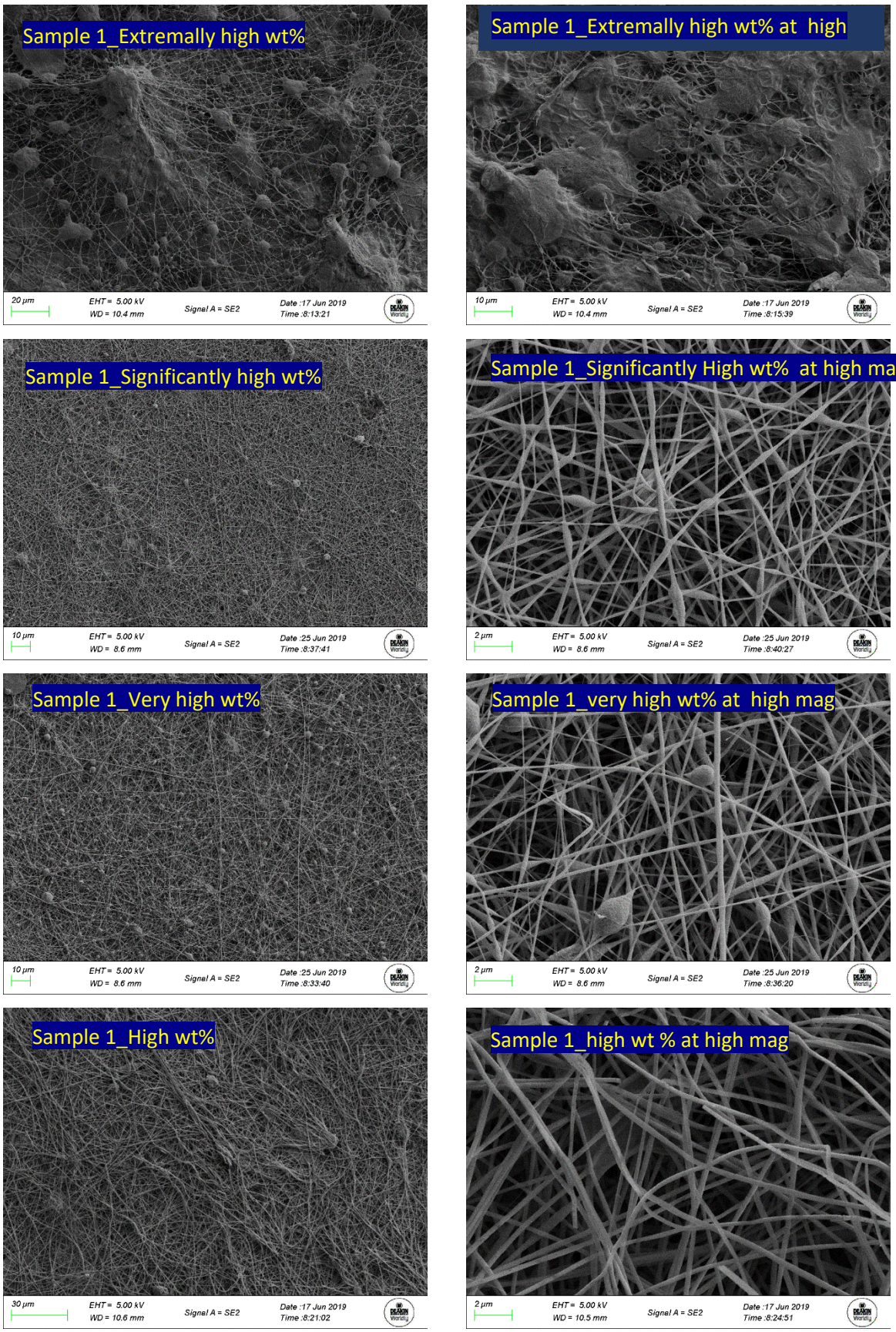

Figure 23 SEM images of Sample 1/PAN electro-spun mats with different Sample 1 contents

Similar to Sample 1, adding some PAN into the spinning dope resulted in formation of very thin fibres in the electro-spun mat. Adding more PAN into the dope resulted in nano-fibre with beads, which can be used in special application such as high surface area nano-fibre mats. Samples with significantly high weight fraction and high weight fraction, formed perfect electro-spun mats with less beads and more uniform nano-fibre structure.

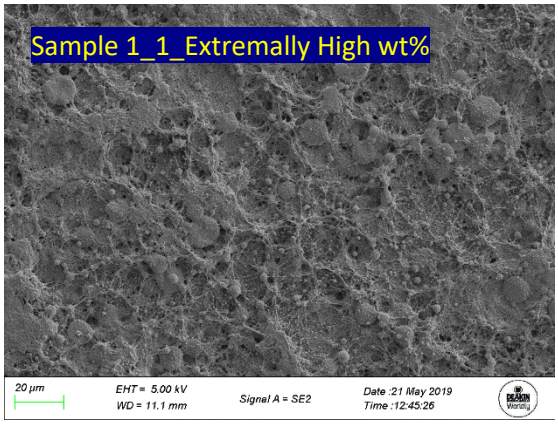

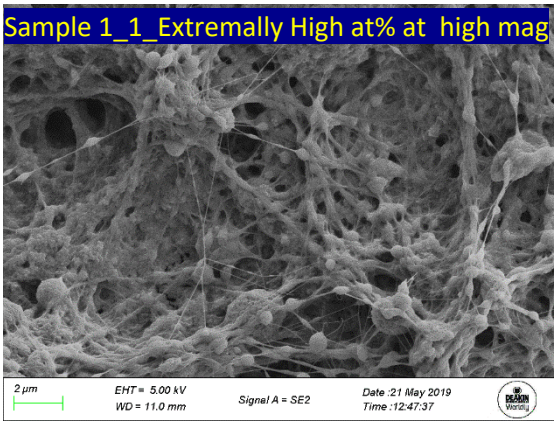

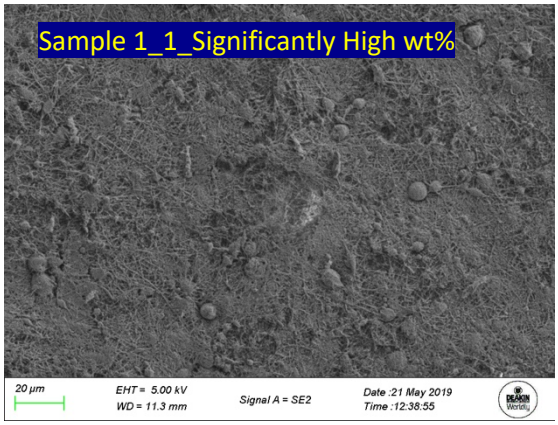

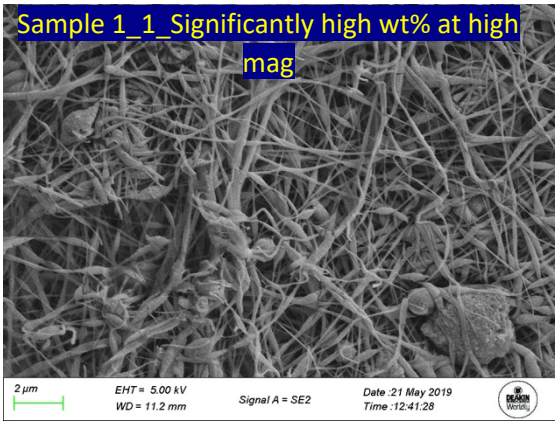

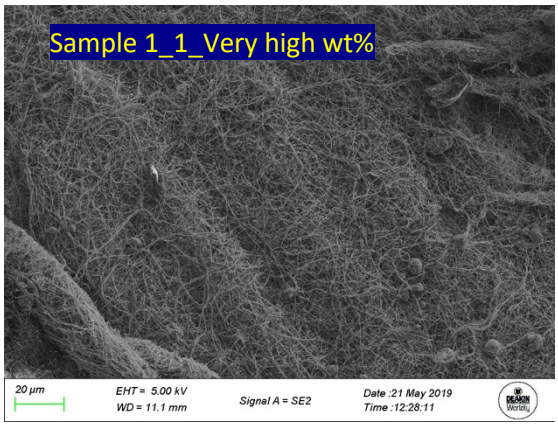

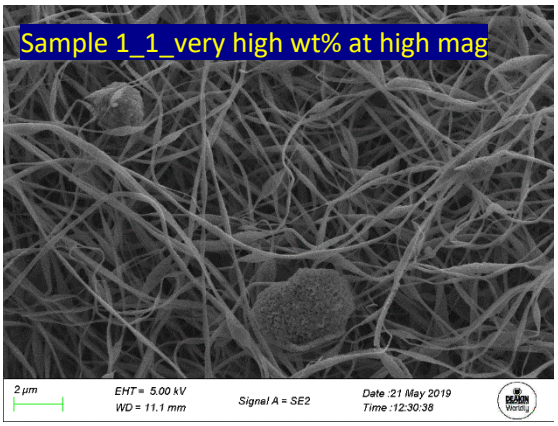

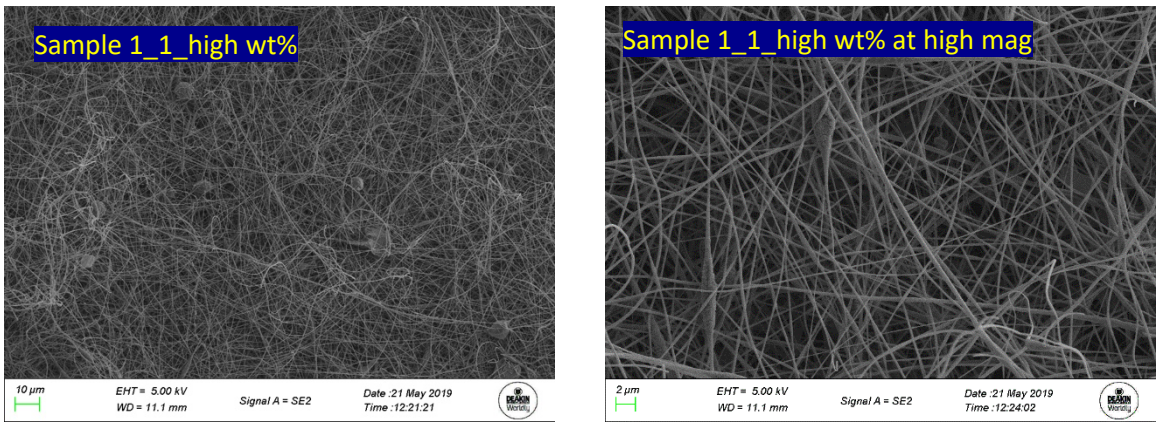

Figure 24 SEM images of Sample 1_1/PAN electro-spun mats with different Sample 1_1 content

As shown in Figure 24, except for the extremally high weight fraction, which contains a few random fibres in the structure, all other samples contain an acceptable amount of nano-fibres in their structure and therefore can potentially assessed for energy storage and/or contamination removal applications. Sample 1_3 was also mixed with PAN for preparing electro-spinning dope and were spun successfully on the collector. Figure 25 shows SEM images of nano-fibre mats were prepared using Sample 1_3.

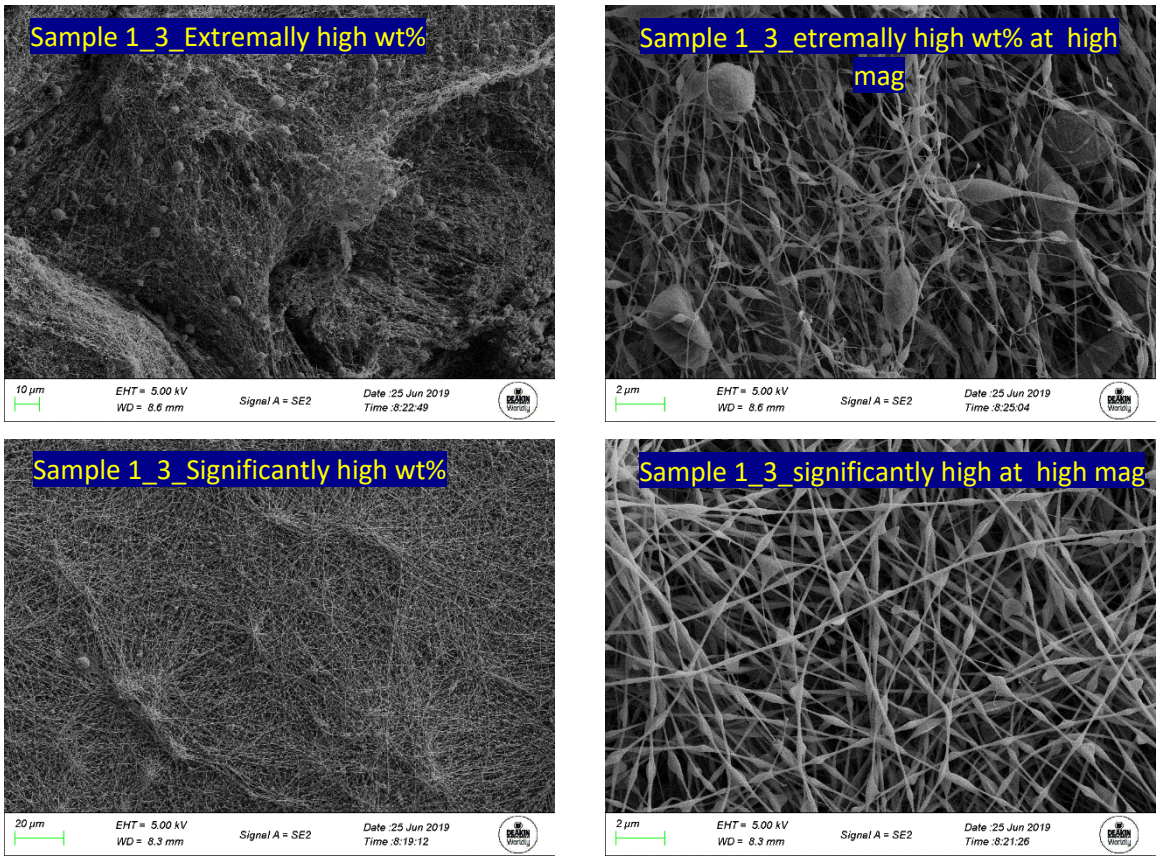

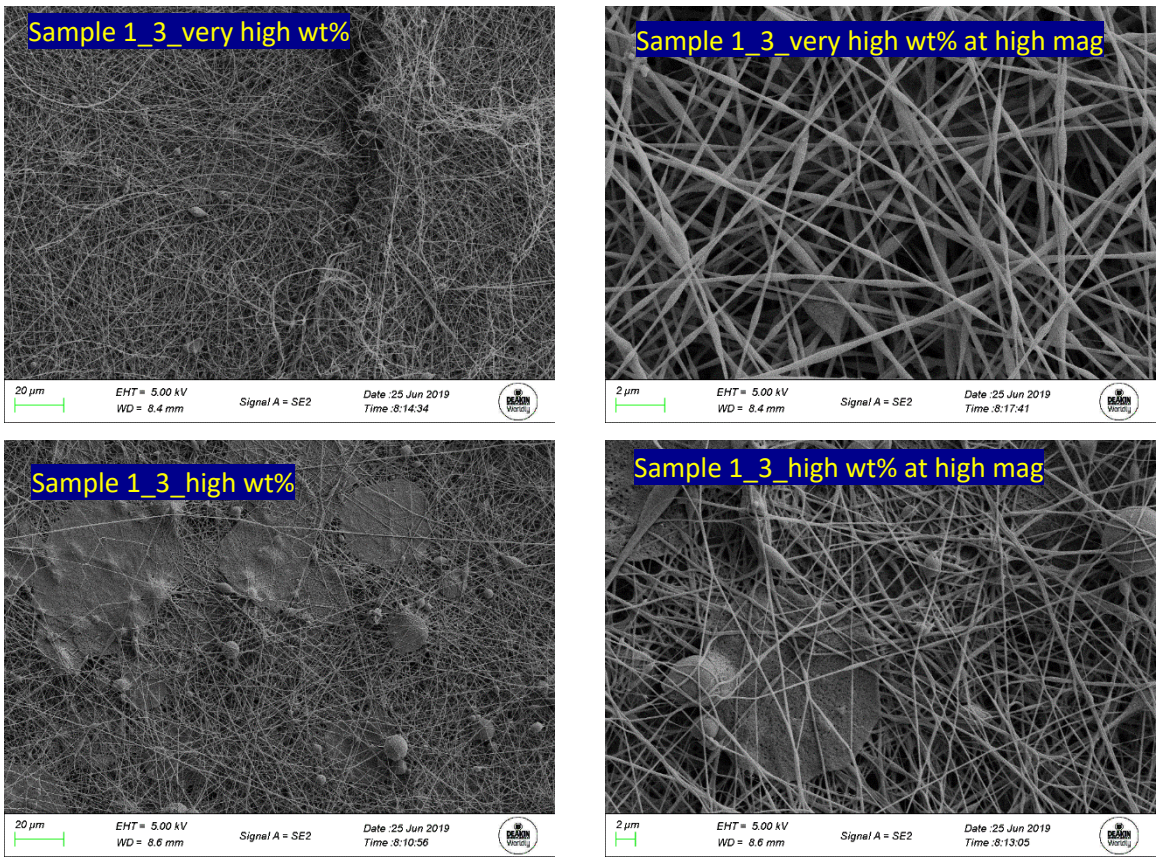

Figure 25 SEM images of Sample 1_3/PAN electro-spun mats with 20 to 80wt% of PAN polymer

As shown in Figure 25, formation of nano-fibres with beads can be clearly seen even at very high concentration of Sample 1_3. Based on SEM images, all Sample 1_3 formed nano-fibre mat, demonstrating there is high compatibility of this specific sample with very low amount of PAN polymer. However, Sample 1_3 showed a very poor dispersion in solvent and a lot of Sample 1_3 patches on nano-fibre mat are observed even at reasonable proportion of Sample 1_3. in the blend.

Figure 26 shows SEM images of electro-spun samples for Sample 2-PAN blends. Interestingly, adding only a little PAN to the spinning dope showed some formation of fibres with beads as presented in Figure 26. By increasing PAN content, the bead formation was reduced, and we obtained roughly uniform fibres with sufficient PAN in the blend.

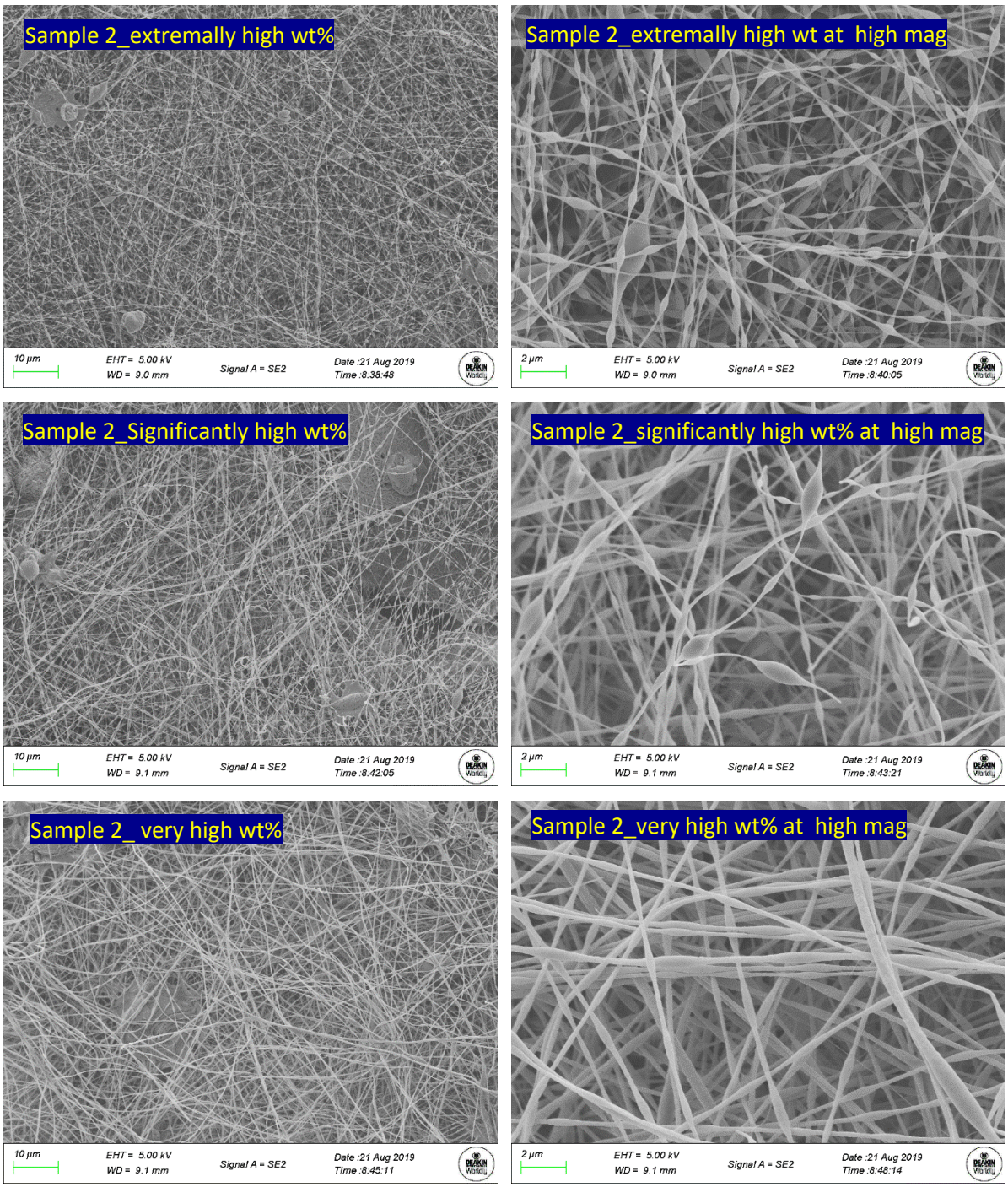

Figure 26 SEM images of electro-spun 100% Sample 2 and Sample 2/PAN polymer blends

Since the aim of electro-spinning experiments is to observe compatibility of PAN and different samples in mixing and forming fibres, we conclude Sample 2 shows higher compatibility in forming fibres at lower PAN concentration compared to other lignite derivatives.

As we mentioned in the experimental procedure, the main outcome of electro-spinning experiment is to investigate compatibility of lignite derivatives in fibre formation process and screen some potentially wet-spinnable samples for wet-spinning application. Sample 1_1 and Sample 2 showed stable mixtures in the solvent and were easily converted to fibres, even at very low PAN

concentrations. They can be therefore suitable candidates for preparing wet-spun fibres. In comparison, Sample 1 and Sample 1_3 was not chosen due to different processing disadvantages. Since processing a liquid fibre into carbon fibre is not possible, liquid Sample 1 has not been considered for wet-spinning trials. A liquid sample, leaches out of fibres in multiple baths, sticks to rollers and heated godets and subsequently fuses the filaments into each other. Moreover, it is not possible to convert a sample with some liquid content in the stabilisation ovens and carbonisation furnaces as it forms flammable fumes. Therefore, Sample 1_1 sample was selected as the first candidate for making a spinning dope. Contrarily, Sample 1_1 is a proper solid material and it results in making dry fibres. However, it has very poor solubility in the solvent and subsequently, a heterogeneous dispersion in the spinning dope. Homogeneity of dope is the key to spin homogeneous fibres with uniform physical and high mechanical properties.

5.3 Wet-spinning of selected VL derivatives

Figure 27 shows dark brown colour of a Sample 1_1-PAN wet-spinning dope. 100 filaments fibre tows were dried on a heated godet at the end of wet-spinning process and samples were collected on a cardboard core for further processing. Moreover, blends with a range of Sample 1_1 and Sample 2 contents were successfully spun and prepared for further processing. As a general observation, spinning of lower concentrations of Sample 1_1 and Sample 2 in PAN was straight forward and similar to a normal PAN precursor. In comparison, adding too much % Sample 1_1 or Sample 2 introduced many issues such as unexpected spinneret clogging, fibre breakage, limited plasticity and fibre drawability.

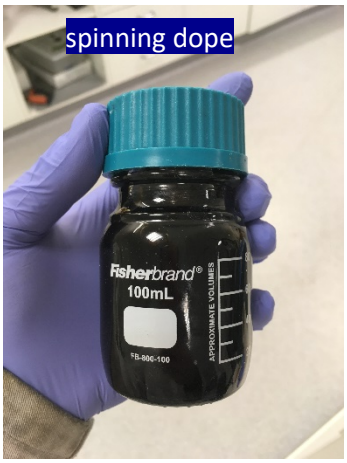

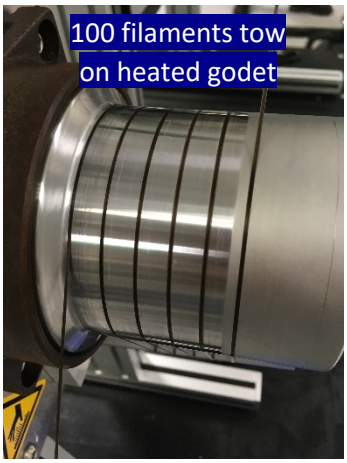

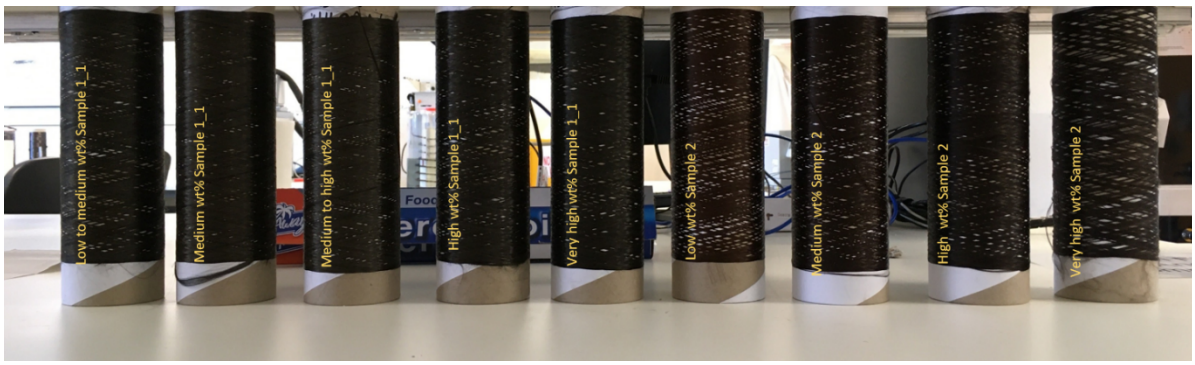

Figure 27 Displaying the wetspun CF precursor with varying load fraction of Sample 1_1 and Sample 2

wet-spinning of blends with more Sample 1_1 or Sample 2 were trialed but, fibres were too brittle to pass through the baths and to be collected on a core.

5.4 Mechanical properties of the fibres

To find a statistically meaningful result, mechanical properties of 25 randomly selected single filaments from each tow were tested using the Favimat machine. Physical and mechanical properties of all wet-spun fibres are shown in Table 3.

Table 3 Mechanical properties of wet-spun PAN/Sample 1_1 and PAN/Sample 2 fibres

Sample	*Elongation (%)*	*Diameter (um)*	*Tensile strength (MPa)*	*Tensile modulus (GPa)*
Control PAN	12.5	12.01	550	11.64
Minimum wt% Sample 1_1	8.95	23.83	310	12.15
Low wt% Sample 1_1	8.96	24.23	300	11.92
Low to medium Sample 1_1	10.34	21.34	265	9.59
Medium wt%% Sample 1_1	10.18	17.44	230	8.54
High wt%% Sample 1_1	6.58	16.72	0.22	9.28
Very high wt%% Sample 1_1	6.95	17.79	0.18	8.06
Low wt%% Sample 2	12.26	17.20	0.27	9.75
Medium wt% % Sample 2	9.40	17.22	0.25	9.57
High wt%% Sample 2	9.90	19.53	0.22	9.21
Very high wt% Sample 2	5.76	22.66	0.13	7.17

As it is shown in Table 3 by adding Sample 1_1 into the spinning dope, elongation and tensile strength of fibre samples were reduced, because of the small draw ratio of the wet-spinning process. Because the initial blends included very little Sample 1_1, we did not optimise wet-spinning parameters and only prepared two fibre samples. In contrast, blends with more Sample 1_1 were prepared at optimised condition and higher draw ratio. As shown in Table 3, by applying a higher draw ratio, we achieved a higher elongation at break and a narrower fibre diameter.

A closer look at the distribution of elongation of fibres at break gives us more details on differences between Sample 1_1 and Sample 2. As shown in Figure 28, PAN/Sample 2 tows are more

heterogeneous compared to PAN/ Sample 1_1 tow as they are more diverse in elongation at break value. This might be because of poor solubility/dispersion of Sample 2 in the solvent that is used to form fibres. Currently, it is thought that the spinning dope contains large Sample 2 particles which, consequently, reduces homogeneity of fibres.

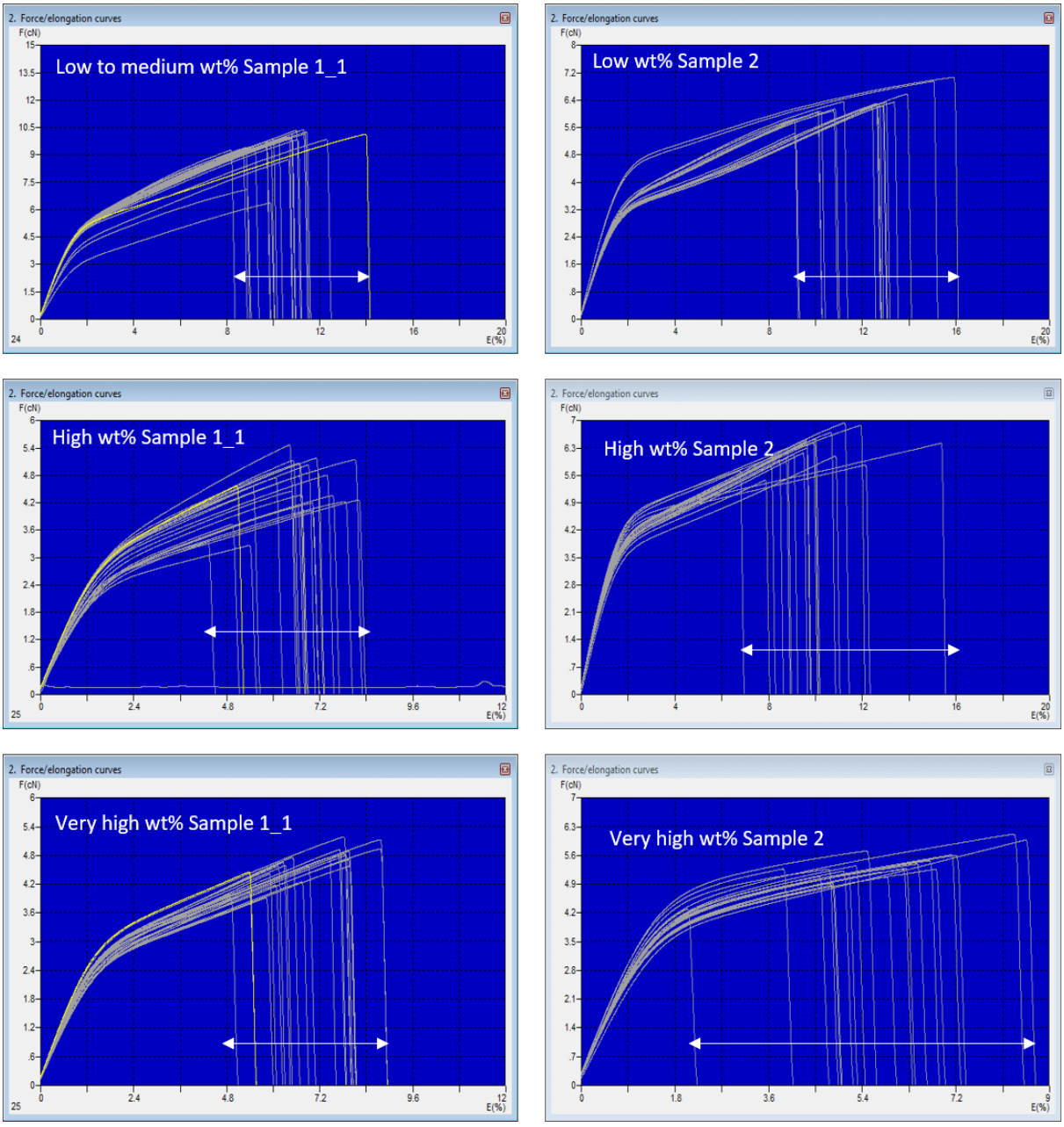

Figure 28 Examples of heterogeneity of elongation of 25 tested filaments from each sample

5.5 Microstructure of fibres

X-ray diffraction of the raw Sample 1_1 and Sample 2 materials and precursor fibres was conducted to investigate the effect of adding two different fillers on the microstructure of the fibres (Figure 29). Based on XRD graphs, Sample 1_1 has more amorphous structure than Sample 2 as it

shows a very broad hump between 10 and 35° Bragg angles. In contrast, Sample 2 shows a recognisable peak around 25°, which is extremely similar to a carbon fibre microstructure. From an XRD point of view, Sample 2 has more similarity to carbon fibre. However, the miscibility issue must be solved before making any firm conclusion.

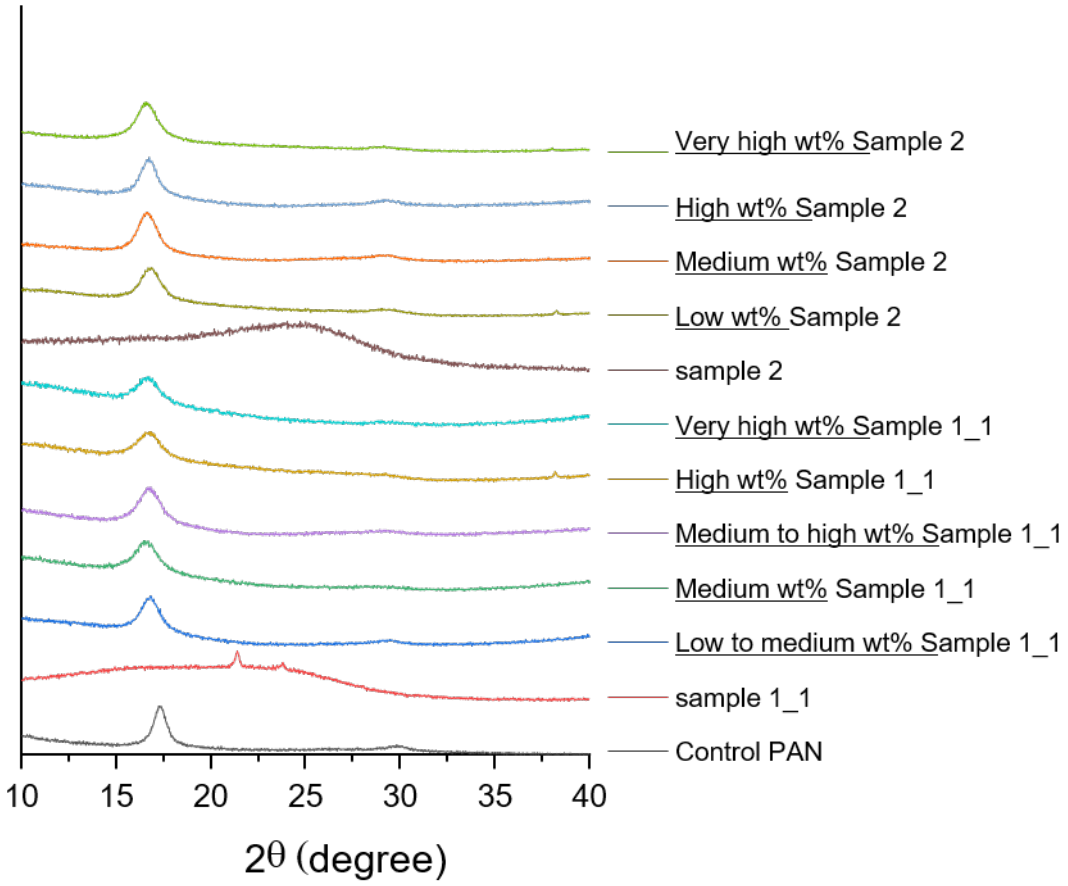

Figure 29 X-ray diffraction pattern of pristine Sample 1_1 and Sample 2 and their wet-spun fibres

5.6 Thermochemical properties of fibres

To investigate the effect of adding Sample 1_1 and Sample 2 on reducing the stabilization temperature of PAN polymer, DSC analysis was conducted on fibre samples. As shown in Figure 30, adding different amounts of Sample 1_1 slightly reduced the peak temperature of reaction. However, this slight reduction may not notably change the required energy for stabilization of composite fibres. In comparison, adding similar amount of Sample 2 did not change the peak temperature of reaction (Figure 31). Comparing the two sets of DSC curves shows that Sample 1_1 may have some synergistic effect on stabilization of the polymer. However, this effect for the PAN/Sample 2 series of samples appears to be negligible.

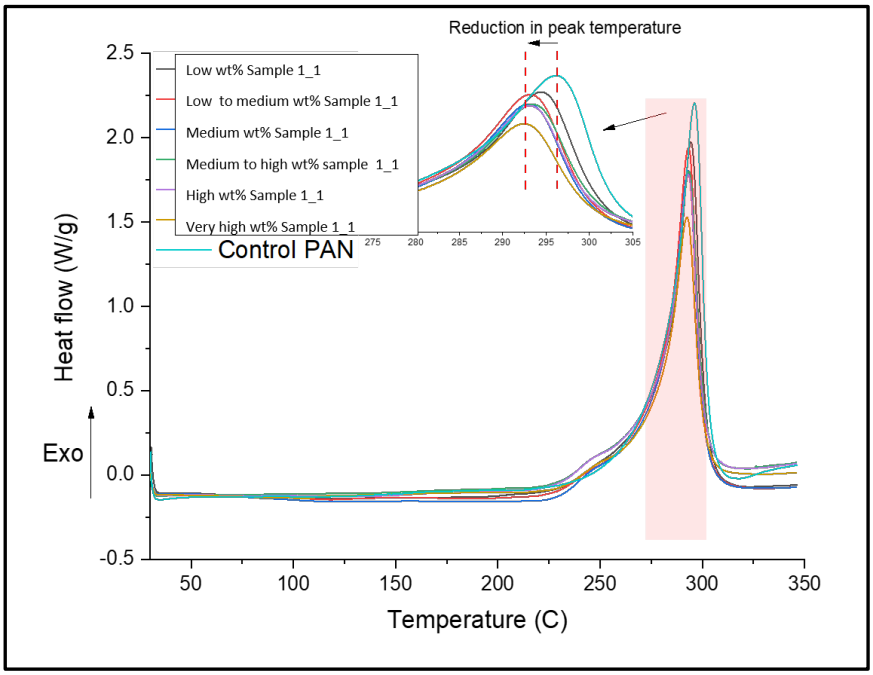

Figure 30 DSC thermogram of PAN/ Sample 1_1 in air atmosphere with a heating rate of 10°C/min

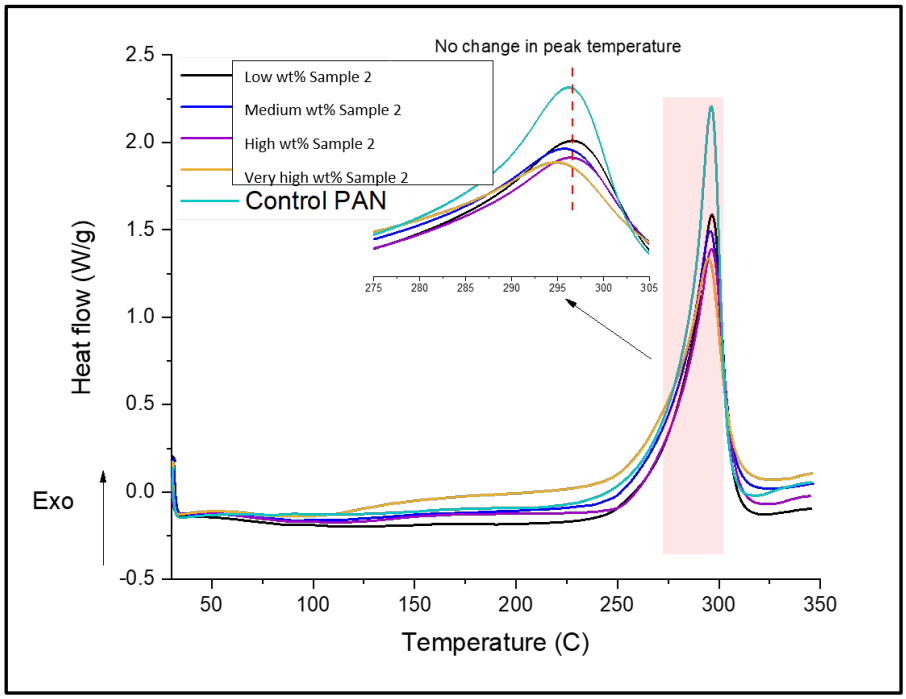

Figure 31 DSC thermogram of PAN/Sample 2 in air atmosphere

A deeper investigation into stabilization of the fibres under tension and in an oven was undertaken by FTIR analysis and it is shown in section 5.8.

5.7 Thermo-gravimetric analysis of fibres

TGA results of PAN/Sample 1_1 fibres are shown in Figure 32 and an increase in weight loss rate by adding more Sample 1_1 is observed in graph; which is in accordance with the DSC results. However, these results do not provide any information about the yield of final product, as carbonization occurs in an inert atmosphere.

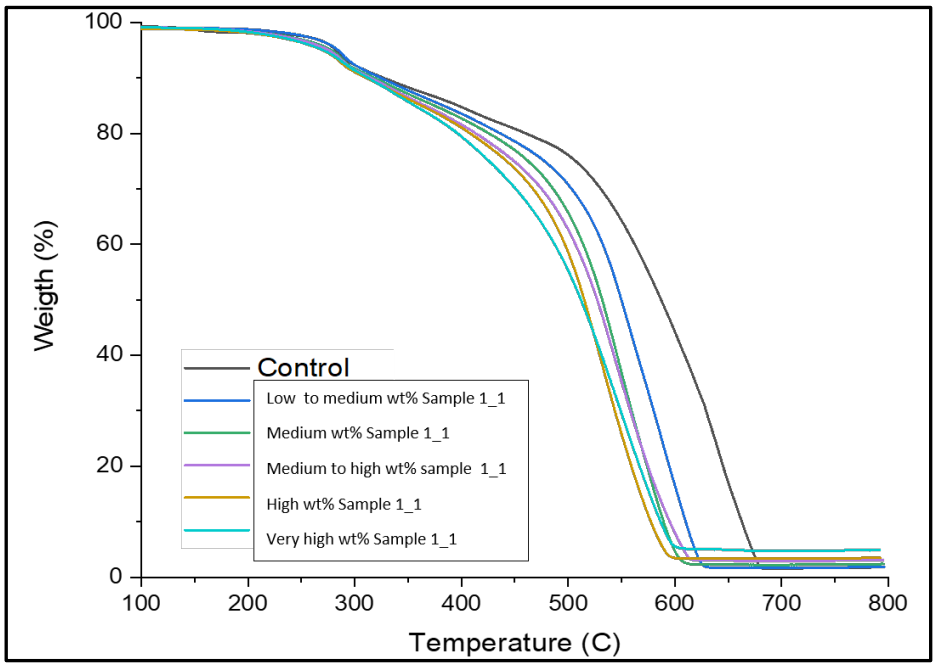

Figure 32 TGA of PAN/Sample 1_1 in air atmosphere

5.8 FT-IR spectroscopy and extent of stabilization reaction

Stabilization of first set of samples in air was completed and Table 4 shows EOR values of all samples. The preferred EOR value for stabilised precursor fibre is between 0.6 and 0.7 and these fibres withstand carbonization at high temperature. Lower EOR values increase the risk of releasing flammable fumes in the carbonization stage. In contrast, higher EOR values reduce reactivity and stabilised chains at higher temperature and does not allow them to form large graphitic structure. As a result, a brittle carbon fibre with lower mechanical properties will be produced from 'over-stabilised' fibres.

As shown in Table 4**,** stabilising fibres at high temperature resulted in very high EOR value which is not suitable for carbonization. To bring the EOR value down to an acceptable value samples were stabilised at different temperatures.

Table 4 calculated EOR values of precursor fibres for different stabilization temperatures

Sample	EOR (%)	SD	Sample	EOR (%)	SD
Control Low temperature stabilization	69.70	1.04	Control low temperature stabilization	69.70	1.04
			Low wt% Sample 2 Low temperature stabilization	58.22	0.92
Low to medium wt% Sample 1_1 Low temperature stabilization	68.53	2.20			
medium wt% Sample 1_1 Low temperature stabilization	69.47	1.56	Medium wt% Sample 2 Low temperature stabilization	61.94	0.68
Medium to high wt% Sample 1_1 Low temperature stabilization	68.72	1.12			
High wt % Sample 1_1 Low temperature stabilization	67.75	0.86	High wt% Sample 2 Low temperature stabilization	60.89	2.17
Very high Sample 1_1 Low temperature stabilization	67.33	0.23	Very high wt% Sample 2 Low temperature stabilization	57.66	2.03
Control 245	71.51	1.98	Control 245	71.51	1.98
			Low wt% Sample 2 high temperature stabilization	73.73	0.52
Low to medium wt% Sample 1_1 high temperature stabilization	71.45	1.84			
Medium wt% Sample 1_1 high temperature stabilization	72.03	2.25	Medium Sample 2 high temperature stabilization	71.45	1.31
Medium to high wt % Sample 1_1 high temperature stabilization	70.66	1.15			
High wt % Sample 1_1 high temperature stabilization	70.52	1.14	high wt% Sample 2 high temperature stabilization	73.47	0.75
very high wt% Sample 1_1 high temperature stabilization	70.66	0.99	very high wt% Sample 2 high temperature stabilization	74.83	0.97
Control very high temperature stabilization	80.09	0.82	Control very high temperature stabilization	80.09	0.82
			low wt% Sample 2 high temperature stabilization	76.54	0.40
Low to medium wt% Sample 1_1 high temperature stabilization	78.25	NA			
medium Sample 1_1 high temperature stabilization	76.29	1.91	medium wt% Sample 2 high temperature stabilization	76.06	1.85
medium to high Sample 1_1 high temperature stabilization	78.18	1.12			
high wt% Sample 1_1 high temperature stabilization	78.09	0.70	high wt % Sample 2 high temperature stabilization	76.91	1.42
very high Sample 1_1 high temperature stabilization	78.43	0.58	very high wt% Sample 2 high temperature stabilization	76.43	0.77

A comparison between EOR values of stabilised control, Sample 1_1 and Sample 2 fibres are shown in Figure 33 and Figure 34, respectively. As discussed before, Sample 1_1 fibre showed higher reactivity than Sample 2 fibres at a certain stabilisation temperature. The same response to temperature was observed for Sample 2 fibres in DSC analysis. As it was shown in previous sections, a notable reduction in reaction peak temperature was observed for Sample 1_1 fibre, while no change in peak temperature was recorded for Sample 2 fibres

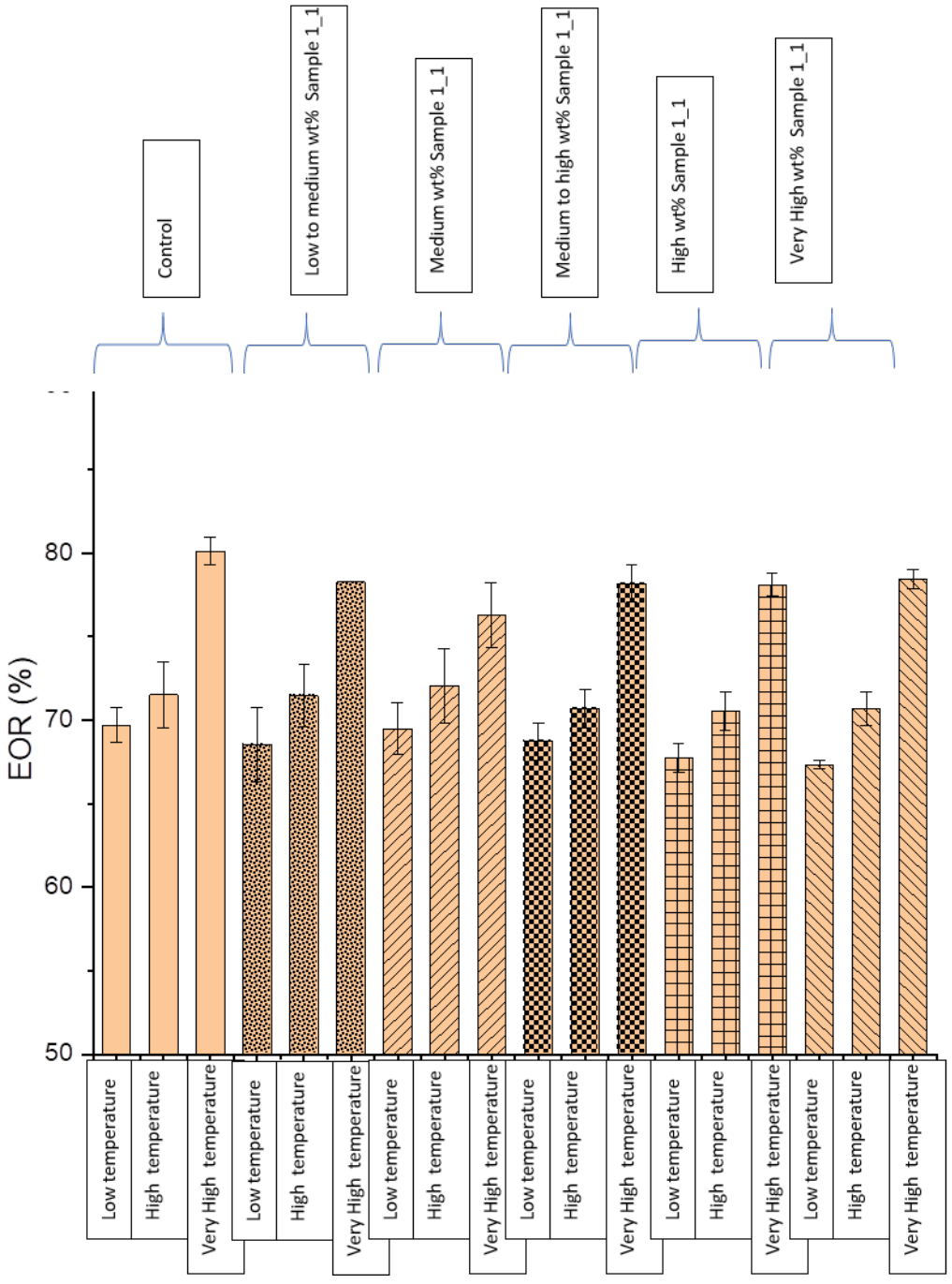

Figure 33 EOR values for stabilised control and Sample 1_1 fibres at three different temperatures

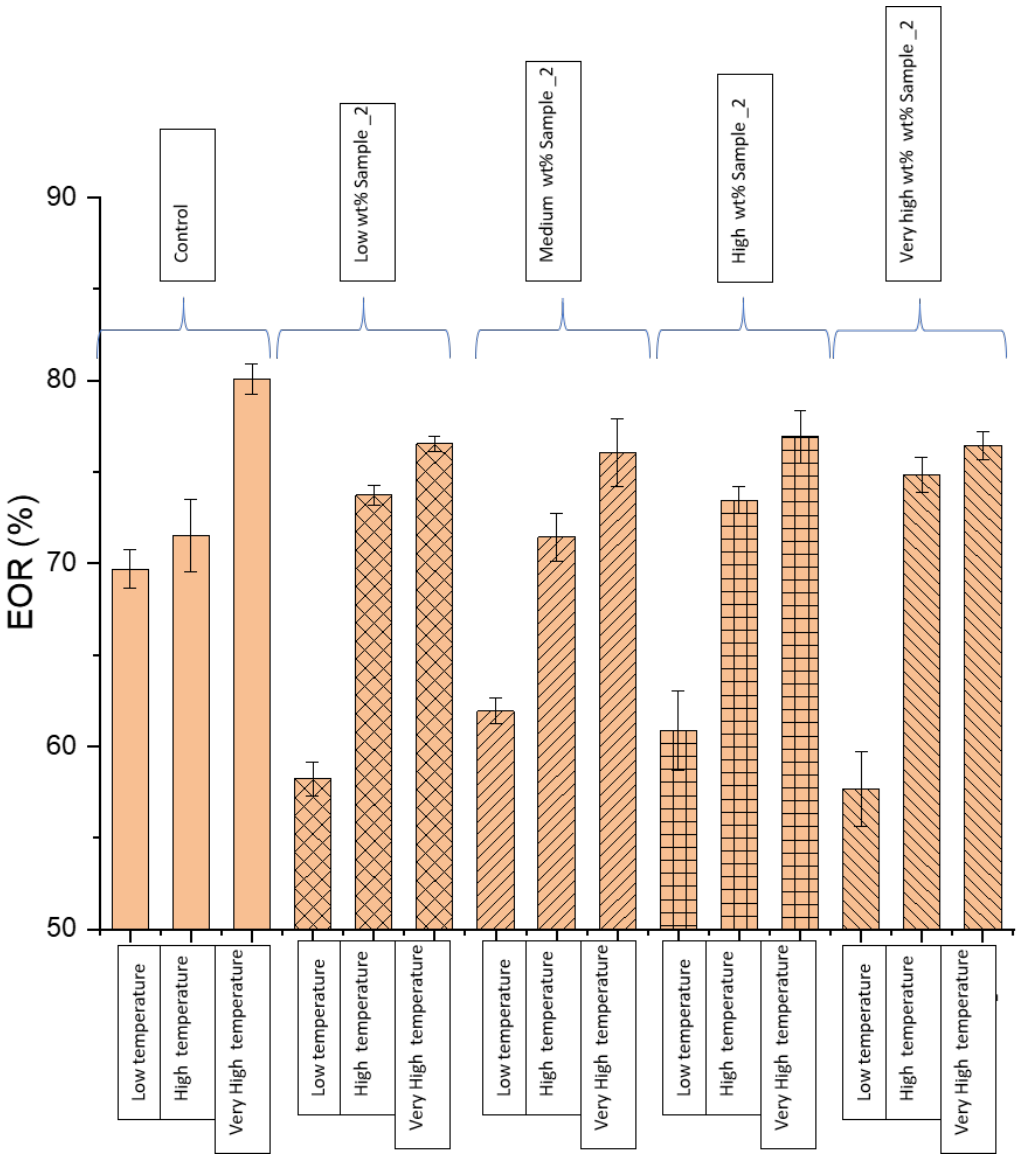

Figure 34 EOR values for stabilised control and Sample 2 fibres at three different temperatures

5.9 Optimization of stabilization and carbonising the stabilized fibre

Carbonisation of stabilized fibre is referred as either low temperature carbonisation or high temperature carbonisation. In the current work, all the carbonisation processes were conducted at low temperature; therefore, the obtained fibre is said to be low temperature carbonised fibre (LT CF). The mechanical properties of LT CF are found to be poor due to less developed 2D planes and poorly aligned crystals along the axis of fibres. LT carbonisation is highly preferred for feasibility studies of carbonisation ability of new combinations of precursors at smaller tow size (<1000 tow). It is well established that stabilization is one of the most important steps in the development of CF. As noted above, higher EOR values can be detrimental to the final carbon fibre properties. Apart from resident time and temperature, tension is another important parameter which is essential to impart alignment of graphitic structure along the carbon fibre axis. In this context, temperature, residence time and tension were found to be important parameters to obtain CF with high mechanical properties and well

aligned graphitic structure. Based on study of EOR and stabilization temperature, the developed CF precursors have been further carbonised with varying tension on the fibre shown in Figure 35. As observed in Table 5, only some lignite samples were successfully carbonised and samples with high amount of lignite materials failed to withstand tension during carbonisation process. It was observed that the fibres with high weight fraction of Sample 1_1 or Sample 2 became very brittle and were continuously breaking under tension.

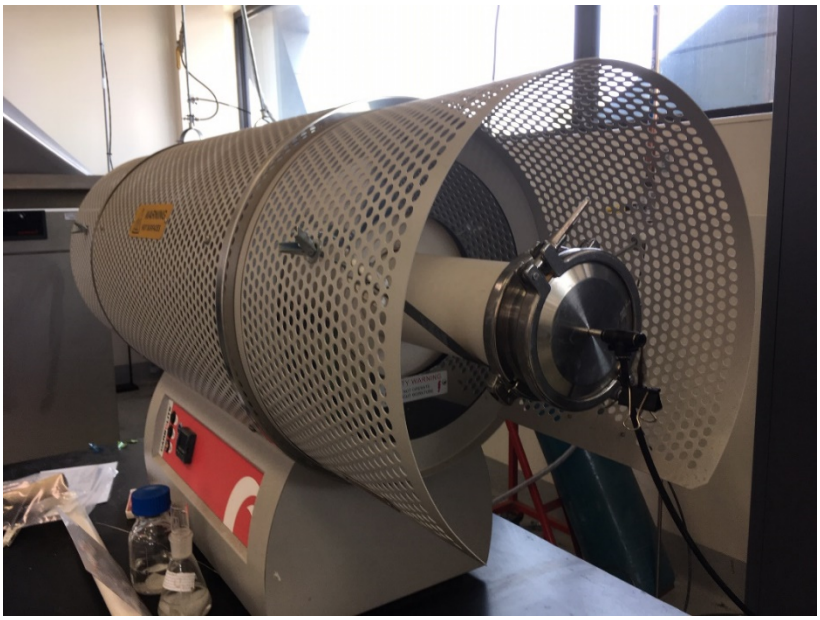

Figure 35 Carbolite Tube furnace for carbonisation of stabilized fibre

Table 5 . Mechanical properties evaluation of carbonised fibre with different weight fractions

Testing order	Sample	Tensile strength (MPa)	Tensile Modulus (GPa)	Description
1	**Low to medium wt%_Sample 1_1**	206.5	33.8	First two samples failed to carbonise
2	**Medium wt %_Sample 1_1**	248.12	59.12	Sample failed to carbonise
3	**Low wt% _Sample 2**	446.87	43.81	Carbonised successfully but the fiber was stabilized at low temperature
4	**Medium wt %_Sample 2**	315.00	68.02	Carbonised successfully but stabilized at high temperature

6. Project Extension

At the completion of the 12-month project, project team managed to demonstrate that a satisfactory precursor fibre can be produced using a high concentration of Sample 2, but to this point

carbonisation was only accomplished for fibres containing medium wt% Sample 2. A three-month extension was granted to allow the project team to build on this success and target production of carbon fibres using high wt% Sample 2. This section of the report deals with the results obtained during the project extension. The project extension was hampered by the COVID-19 disruption and as a result of the restrictions, both Deakin and Monash Universities were operating at reduced capacity and with only limited access to the labs.

6.1 Preparation of lignite derivatives

This section is redacted from this public report.

6.2 Fibre spinning and optimization of CF processing parameters

As mentioned previously, some of the wet-spun lignite fibres did not able to survive the carbonisation process and broke along their length. To allow the fibre to successfully undergo carbonisation process and based on analysis of broken fibre during carbonisation process, a new stabilization profile was employed. It is believed that inclusion of lignite possibly changes the internal structure of PAN which may need higher stabilization temperature with increased residence time. In this context, the remaining precursor fibres stabilized using the new stabilization profile at a higher temperature for a longer time. Despite the less promising mechanical performance of Sample 1_1 fibre compared to Sample 2 fibres (Table 5). Fibres containing, range of proportions of Sample 1_1 were also carbonised to study the difference between mechanical properties of Sample 1_1 and Sample 2 based fibre. The EOR values for fibres stabilized using the new stabilization profile were calculated and are reported in Table 6. As seen in Table 6, the increasing weight fraction of Sample 2, increases the EOR values, though the calculated EOR value is found to be very high compared to the accepted EOR value of 100% PAN fibre. However, it was interesting to see effect of higher EOR values on carbonisation. As illustrated in Table 6, all the fibres survived the carbonisation and applied tension. Almost all the fibre did not undergo any kind of breakage during the entire process of carbonisation. A similar process utilized for carbonisation o Sample 1_1 fibre failed during the previously reported process.

6.2.1 Wet-spinning and processing of Sample 3

The next plan was to wet-spin and convert Sample 3 into carbon fibre. The work involves the development of precursor fibre containing a large proportion of Sample_3 in the Sample _3-PAN blend. As a standard process of dope preparation (Figure 36-a), the first step involves the dispersion of Sample 3 in solvent via bath sonication followed by mechanical stirring by adding PAN in the solution. In the context of Sample 3, analogous method has been employed to prepare dope, but the dope obtained showed visible agglomerates. Such agglomerates did not allow continuous filament forming during the spinning process and subsequently resulted in severe fibre breakage, in addition

to spinneret blockage. The analysis of the dope and broken fibre have demonstrated that bath sonication did not effectively disperse and reduce the particle size. Therefore, it was determined that an alternative method must be employed to reduce the Sample_3 particle size before dispersing it in the solvent as illustrated in Figure 36 (b). This new method gave dope with improved flowability and without any visible agglomerates. The prepared dope facilitated the development of wet-spun fibre as delineated in Figure 36-b. Taking advantage of the previously gained experience on stabilization temperature and residence time, wet-spun Sample 3 fibres were stabilized at a higher temperature and longer residence time. The obtained EOR values and mechanical properties of Sample 3 carbonised samples are shown in Table 6.

Table 6 EOR value for the stabilized fibre at 270℃

Samples	EOR (%)	SD (%)	Tensile Strength (MPa)	Tensile Modulus (GPa)
Low wt% Sample 2	67.42	6.02	446	43.81
Medium wt%- Sample 2	69.08	1.58	315	68.02
High wt% - Sample 2	70.80	4.20	190	62.64
Very High wt% Sample 2	79.52	4.71	60-150	37.05
Very high wt%-Sample 3	76.80	2.60	130	30.15
Low wt% -Sample 1_1	-	-	180	54.20
Very high wt% Sample 1_1	-	-	140	39.00

It is important to understand the effect of stabilization and carbonisation process parameters on the quality of CF. The fibre processed under the optimized/modified conditions developed earlier were evaluated qualitatively by folding/rolling around smaller diameter bobbins. The result has been demonstrated in Figure 37(a-c). As indicated in Figure 37(a), carbon fibre containing a small amount of Sample 1_1 CF stabilised under the original conditions gave many broken ends and it was challenging to fold them. However, under the modified conditions, even fibre containing more of Sample 2 in the blend was easier to handle and far more flexible compared to all other fibres processed under the previous carbonisation condition.

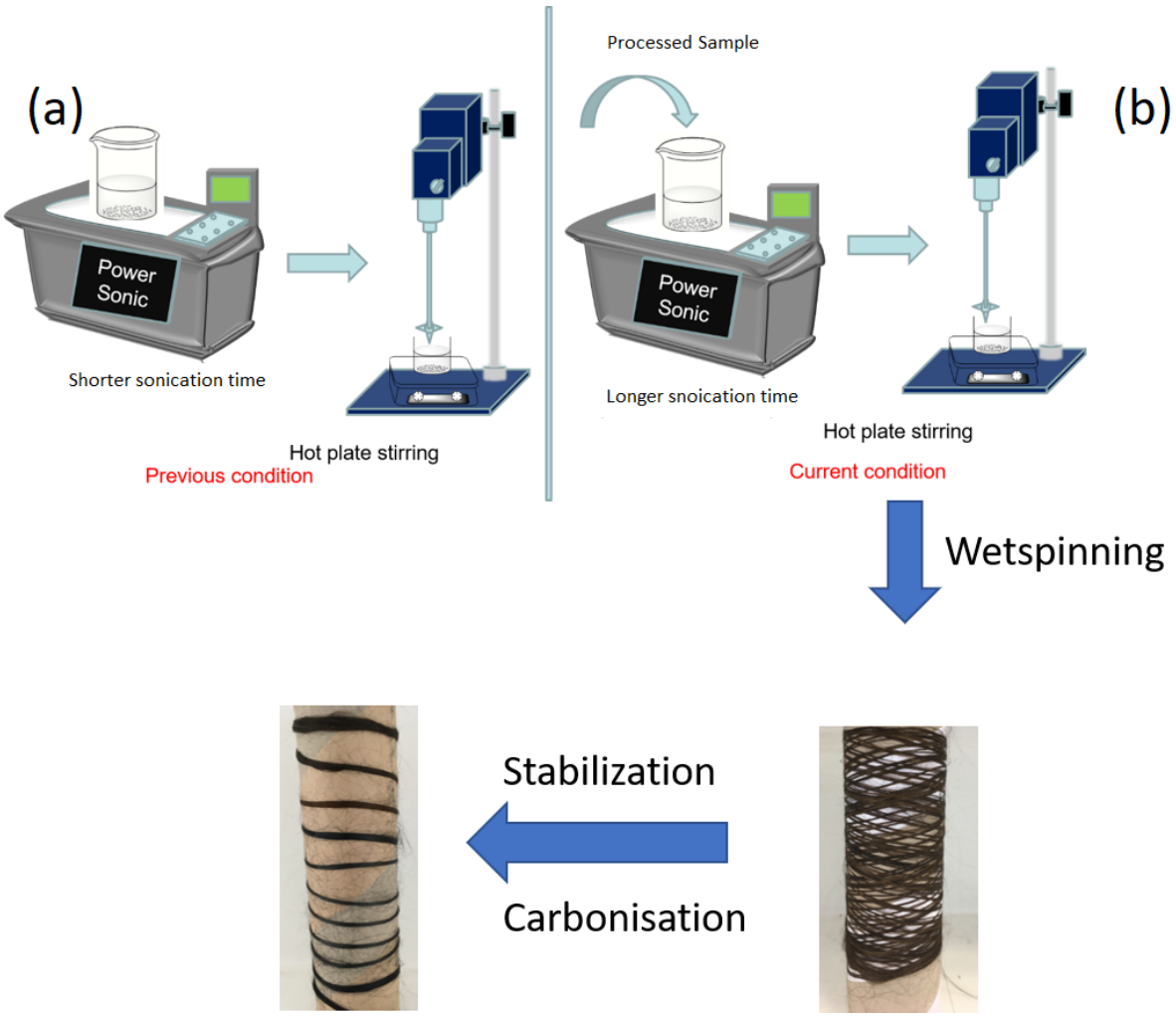

Figure 36 (a) preparation of dope as standard method (b) modified method of dope preparation by processed sample as additional step

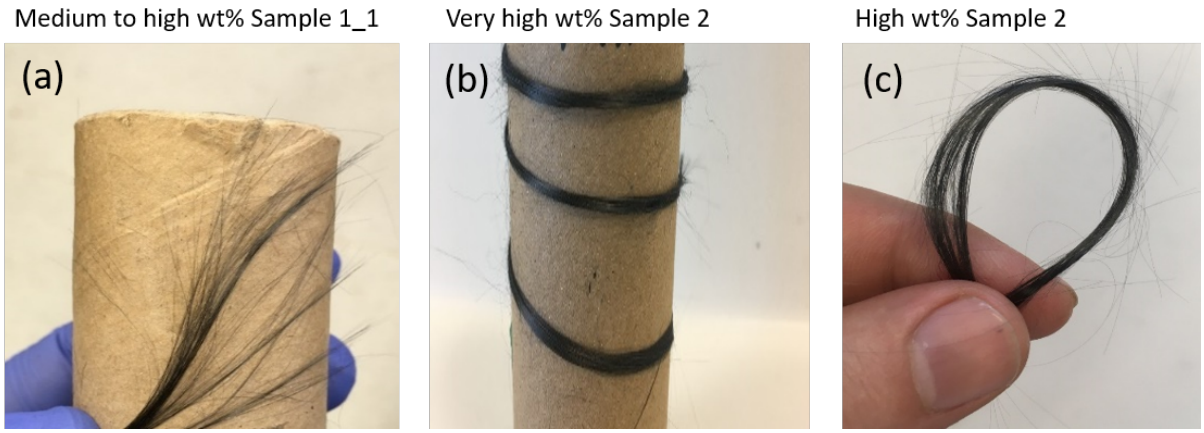

Figure 37 (a) Demonstrating broken ends and nonflexibility of a Sample 1_1-PAN blend CF with little sample one, processed under old stabilization condition (b) and (c) demonstrating the flexibility and easy handling of Sample 2-PAN blend CF samples containing more Sample_2 under optimized stabilization condition

To demonstrate the importance of current work, Figure 38 demonstrates the mechanical properties of low temperature CF, developed in our team from commercially available PAN precursor

compare with the results developed of the current work (Nunna, Maghe, Fakhrhoseini, Polisetti, & Naebe, 2018). As illustrated in Figure 38, the mechanical properties of obtained Sample 2 are very close to the commercial LT fibres. It is believed that further process optimization may facilitate further improvement in mechanical properties. It is envisioned that if work on Sample 2 is extended further for processing with higher tow size, higher carbonisation temperature will presumably pave the way for developing new class of CF precursor fibre.

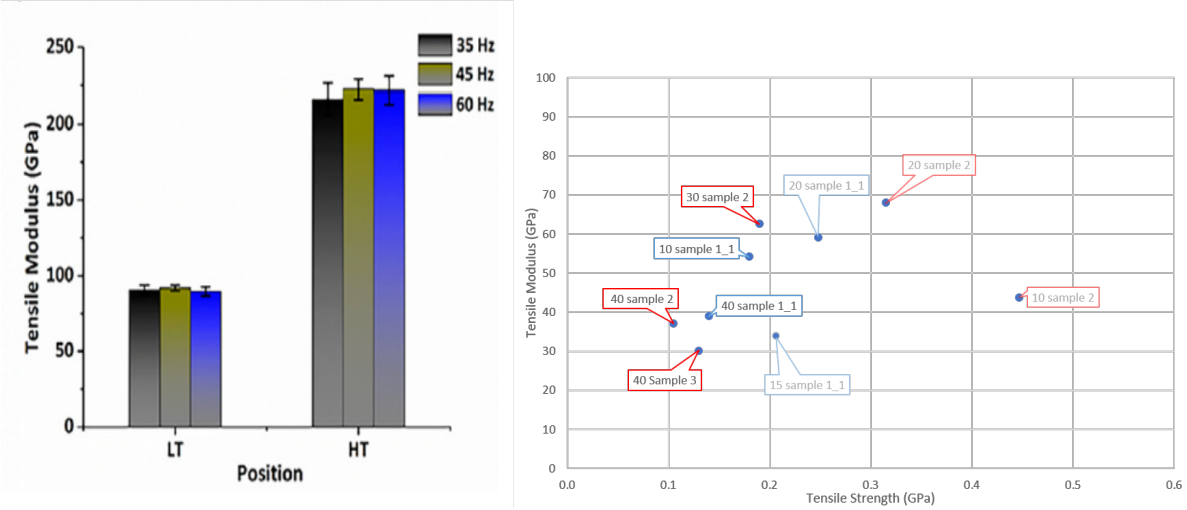

Figure 38 Comparison of current work with other low temperature CF developed from commercial PAN precursor

6.2.2 Raman Analysis of the CF

Raman spectroscopy is an important tool to characterise the most important feature of G (graphitic) and D (disordered induced) bands in carbon fibre. Such features are generated due to the C–C bonds stretching vibrations available in carbon-based materials like carbon fibre. PAN based carbon fibre do not exhibit entirely graphitic structure and contains disordered turbostatic carbon. Therefore, the relative intensities of the D- band and G-band are obtained in RAMAN spectra of such carbon fibre are primarily influenced by the size of the sp2 graphitic carbon structure, the ratio of sp2/sp3 carbon, etc. In the current work, the I_D/I_G ratio of Sample 2-based CF was obtained in the reported range and indicates partial augmentation of the graphitic structure with increasing weight fraction of Sample 2 for low temperature CF as illustrated in Figure 39. In contrast, the reinforcing Sample 1_1 has imparted disruption to the graphitic structure in the developed CF. Though, Sample 1_1 has demonstrated better spinnability and mechanical properties as precursor fibre, but the obtained CF do not exhibit such well aligned graphitic structure and hence demonstrated poorer mechanical properties. Therefore, Sample 2 is observed to be a prominent alternative for the development of carbon fiber precursor material compared to Sample 1_1.

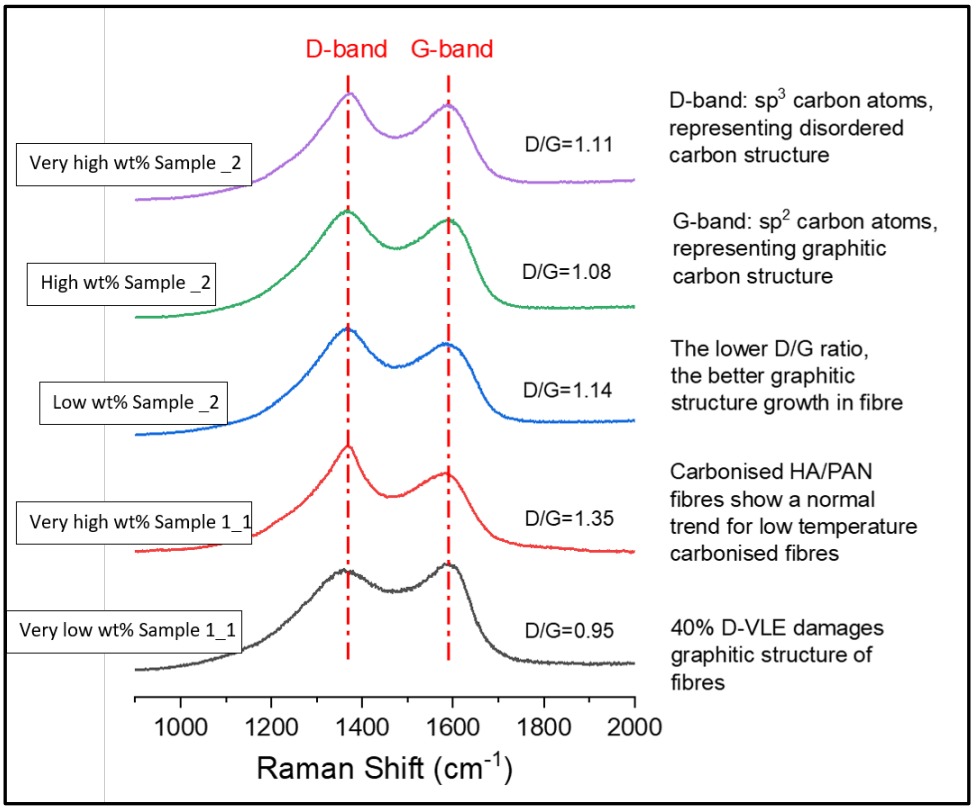

Figure 39 RAMAN analysis of the developed CF

Conclusions

The properties of the materials tested varied with regard to elemental analysis, density, textural properties and structural parameters such as aromaticity. The effect of pyrolysis in an inert atmosphere or in air/N_2 (1/1) also varied significantly. The volatility should ideally be low to increase the yield of the final product. As expected from its distinct chemical structure Sample 6 was less volatile than any other material tested and so from this point of view Sample 6 would be expected to be a good prospective precursor material. Of the materials tested for CF production, Sample 2 would be expected to be better than Sample 1_1 because of its different elemental analysis and high carbonization yield. Sample 3 had lower carbonization yield than Sample 2, perhaps because of its chemical structure and undesirable analytical characteristics; thus it would be expected to be less suitable for CF production. Therefore, of the materials tested, the Sample 2 would appear to be the best CF precursor on account of its physico-chemical properties in conjunction with a suitable solvent.

Precursor spinning and thermal conversion of fibres provided higher thermal stability for Sample 2-PAN and Sample 3-PAN composites, as they easily converted to stabilised fibres and were subsequently successfully carbonised. In comparison, the thermoplasticity of Sample 1_1 and its low-temperature phase transformation question its potential as a useful CF precursor material.

Future Scope

PAN based fibre was first invented in 1959 and since then CF is continuously finding its global market in many applications like automobiles, aviation, space and many more. The global demand of CF is continuously increasing but its high cost is still a main concern which do not allow the exploitation of its full potential. Although a number of precursors have been exploited in the recent years for the development of low-cost carbon fibre, achieving mechanical properties equivalent to PAN based CF remains a challenge. It is primarily the cost of the PAN precursor that limits the possibility of reducing the overall cost of CF development. Therefore, two main strategies have been employed to counter the high precursor cost (i) develop and evaluate the new alternative to PAN as a precursor material (ii) blending PAN with potentially alternative precursor materials to reduce its overall material requirement of the precursor. The current work has demonstrated the second strategy to reduce the cost of CF production. The findings in this work open the following avenues which might be utilized to define the future direction of the work:

(i) The mechanical and structural analysis of the lignite samples have demonstrated Sample 2 as a potentially better filler for PAN relative to Sample 1_1. The diameter of precursor fibres obtained in this work by wet-spinning technique was noted to be very high so that modification of Sample 2 to give a better mixing and interaction with PAN would be desirable. Therefore, further optimization of wet-spinning parameters is recommended to develop precursor fibre with required fibre diameter (<13µm). In particular, further investigations based on Sample 2 and Sample 3 to optimise their properties so as to make them more suitable candidates for wet-spinning is recommended.

(ii) Modification of the chemistry of Sample_1 to obtain a material which when mixed with PAN will promote the graphitization of the wet-spun fibre.

(iii) Experimental survey to find more suitable solvents for making a mixture of the precursors with PAN for wet-spinning. Particular attention should be directed to polar 'green' solvents.

(iv) Further experiments are necessary to produce a sufficient quantity of Sample 6 for wet-spinning.

(v) The current work exploits the development of precursor fibre with 100 filaments in a tow, which is not sufficient to showcase the actual potential of lignite as filler for PAN. Therefore, it is envisaged that larger tow size must be manufactured and evaluated for CF production.

(vi) The stabilization and carbonisation conditions were optimized for 100 filament system in the current work. However, it is recommended that future trials be conducted using a

commercially relevant state-of-the-art research facility located in Carbon Nexus, to appropriately correlate the structural and mechanical properties of Samples 2 and 3 based CF to various commercially available CF.

(vii) Apart from developing a CF with comparable mechanical properties, it is essential to carry out the detailed cost analysis and effect of reinforcing lignite inclusions on overall cost of CF development.

References

Alcañiz-Monge, J., Cazorla-Amorós, D., Linares-Solano, A., Oya, A., Sakamoto, A., & Hosm, K. (1997). Preparation of general purpose carbon fibers from coal tar pitches with low softening point. *Carbon, 35*(8), 1079-1087. doi: https://doi.org/10.1016/S0008-6223(97)00064-X

Brown, J. K., & Ladner, W. R. (1960). Hydrogen distribution in coal-like materials by high-resolution nuclear magnetic resonance spectroscopy. II. A comparison with infrared measurement and the conversion to carbon structure. *Fuel, 39*, 87-96.

Charlesworth, J. M. (1980). Influence of temperature on the hydrogenation of Australian Loy-Yang brown coal. 2. Structural analysis of the asphaltene fractions. *Fuel, 59*(12), 865-870. doi: http://dx.doi.org/10.1016/0016-2361(80)90036-8

Frank, E., Steudle, L. M., Ingildeev, D., Spoerl, J. M., & Buchmeiser, M. R. (2014). Carbon fibers: precursor systems, processing, structure, and properties. *Angewandte Chemie International Edition, 53*(21), 5262-5298.

Grassie, N., & McGuchan, R. (1972). Pyrolysis of polyacrylonitrile and related polymers—VI. Acrylonitrile copolymers containing carboxylic acid and amide structures. *European Polymer Journal, 8*(2), 257-269.

Hajir Bahrami, S., Bajaj, P., & Sen, K. (2003). Thermal behavior of acrylonitrile carboxylic acid copolymers. *Journal of applied polymer science, 88*(3), 685-698.

Jiang, E., Maghe, M., Zohdi, N., Amiralian, N., Naebe, M., Laycock, B., . . . Annamalai, P. K. (2019). Influence of different nanocellulose additives on processing and performance of PAN-based carbon fibers. *ACS omega, 4*(6), 9720-9730.

Kelemen, S. R., Afeworki, M., Gorbaty, M. L., Sansone, M., Kwiatek, P. J., Walters, C. C., . . . Behar, F. (2007). Direct characterization of kerogen by X-ray and solid-state ^{13}C nuclear magnetic resonance methods. *Energy & Fuels, 21*(3), 1548-1561. doi: 10.1021/ef060321h

Khayyam, H., Jazar, R. N., Nunna, S., Golkarnarenji, G., Badii, K., Fakhrhoseini, S. M., . . . Naebe, M. (2020). PAN precursor fabrication, applications and thermal stabilization process in carbon fiber production: Experimental and mathematical modelling. *Progress in Materials Science, 107*, 100575.

Ko, S., Choi, J.-E., Lee, C. W., & Jeon, Y.-P. (2017). Modified oxidative thermal treatment for the preparation of isotropic pitch towards cost-competitive carbon fiber. *Journal of Industrial and Engineering Chemistry, 54*, 252-261. doi: https://doi.org/10.1016/j.jiec.2017.05.039

Koppers. (June 25, 2012). Coal tar pitch. *SDS ID: 00230086.* Retrieved Feb 18, 2015, from http://chemadvisor.com/Koppers/Database/koppers_austasia/msds/00230/00230086004664403.PDF

Lundin, H. (1931). Determination of water by distillation with liquids heavier than water. I. Tetrachloroethane. *Chemische-Zeitung, 55*, 762-763.

Mollah, M. M., Marshall, M., Sakurovs, R., Jackson, W. R., & Chaffee, A. L. (2016). Attempts to produce blast furnace coke from Victorian brown coal. 3. Hydrothermally dewatered and acid washed coal as a blast furnace coke precursor. *Fuel, 180*, 597-605.

Nunna, S., Blanchard, P., Buckmaster, D., Davis, S., & Naebe, M. (2019). Development of a cost model for the production of carbon fibres. *Heliyon, 5*(10), e02698.

Nunna, S., Maghe, M., Fakhrhoseini, S. M., Polisetti, B., & Naebe, M. (2018). A pathway to reduce energy consumption in the thermal stabilization process of carbon fiber production. *Energies, 11*(5), 1145.

Omnia. (10.08.2018). K-Humate. Retrieved Sep 29, 2020, 2020, from https://www.omnia.com.au/products/k-humate-s100

Oroumei, A., Fox, B., & Naebe, M. (2015). Thermal and rheological characteristics of biobased carbon fiber precursor derived from low molecular weight organosolv lignin. *ACS Sustainable Chemistry & Engineering, 3*(4), 758-769.

Parsa, M. R., Tsukasaki, Y., Perkins, E. L., & Chaffee, A. L. (2017). The effect of densification on brown coal physical properties and its spontaneous combustion propensity. *Fuel, 193*, 54-64. doi: https://doi.org/10.1016/j.fuel.2016.12.016

Qu, W., Liu, J., Xue, Y., Wang, X., & Bai, X. (2018). Potential of producing carbon fiber from biorefinery corn stover lignin with high ash content. *Journal of applied polymer science, 135*(4), 45736.